Revision 1

TYPE 1 FAULTS IN THE YUCCA MOUNTAIN REGION

Prepared for

Nuclear Regulatory Commission
Contract NRC-02-93-005

Prepared by

Center for Nuclear Waste Regulatory Analyses
San Antonio, Texas

November 1996

CNWRA 96-007
Revision 1

TYPE I FAULTS IN THE YUCCA MOUNTAIN REGION

Prepared for

Nuclear Regulatory Commission
Contract NRC-02-93-005

Prepared by

H. Lawrence McKague
John A. Stamatakos
David A. Ferrill

Center for Nuclear Waste Regulatory Analyses
San Antonio, Texas

November 1996

CONTENTS

FIGURES

TABLES

ACKNOWLEDGMENTS

This report was prepared to document work performed by the Center for Nuclear Waste Regulatory Analyses (CNWRA) for the Nuclear Regulatory Commission (NRC) under Contract No. NRC-02-93-005. The activities reported here were performed on behalf of the NRC Office of Nuclear Material Safety and Safeguards (NMSS), Division of Waste Management (DWM). The report is an independent product of the CNWRA and does not necessarily reflect the views or regulatory position of the NRC. We thank Esther Cantu for preparation and Barbara Long for editorial review. Thorough reviews by Charles Connor and Wesley Patrick were greatly appreciated.

Without the excellent cooperation of a number of CNWRA staff, this study could not have been completed. R. Martin processed the fault map data and was instrumental in providing guidance in the use and pitfalls of ARC/INFO. P. Maldonado used Excel to calculate moment magnitudes and peak accelerations. R. Hofmann provided the peak acceleration formula and guidance in its use. E. Cantu prepared the spreadsheet from the Piety (1996) report and the final draft of this report. B. Henderson prepared some of the figures.

QUALITY OF DATA, ANALYSES, AND CODE DEVELOPMENT

DATA: The basic data presented here are from published and nonpublished sources. The data from Piety (1996) is included in a draft U.S. Geological Survey Open-File Report and could be subject to change. All other data are from published sources. Referenced sources should be consulted to determine their level of quality assurance.

ANALYSES AND CODES: Scientific computer codes were used in the analyses contained in this report. ARC/INFO (Version 6.1.1) from Environmental Systems Research Institute, Inc., of Redlands, California, is the Geographical Information System (GIS) software that was used in this analysis. This is commercial software and only the object code is available to the CNWRA. This software is not controlled under CNWRA Technical Operations Procedure "Configuration Management of Scientific and Engineering Codes," (TOP-18). 3DStress, v.1.0, was used in some of the analyses: it was developed by the CNWRA and is under software configuration control at the CNWRA. The spreadsheet Excel, v.5.0, from Microsoft Corporation was used in the analyses. This is a commercial software with only the object code available to the CNWRA.

EXECUTIVE SUMMARY

The technical objective of the Structural Deformation and Seismicity (SDS) Key Technical Issues (KTI) team is to provide an adequate understanding of technical concerns related to tectonic activity of the Yucca Mountain region (YMR). The SDS team is to provide timely prelicensing review and develop the technical expertise necessary for review of a license application for the proposed high-level nuclear waste (HLW) repository at Yucca Mountain (YM). As outlined in the SDS KTI Implementation Plan[1], the ultimate goal of the KTI is to ensure that significant structural deformation and seismicity conditions and hazards are identified, sufficiently understood, and fully considered and appropriately used in evaluations of repository performance. This report specifically relates to SDS KTI subissues concerning data, model validation and verification, alternative conceptual models, and potential for disruption of waste packages, underground openings, and surface facilities/operations.

The Central Basin and Range Province is characterized by a complex system of extensional and strike-slip faults that have been active since the onset of the Cenozoic Era (65 Ma). More than 400 faults within a 100 km radius of the proposed repository site at YM have been identified and mapped. This report identifies those faults that pose significant seismic hazards to overall safety and performance of the proposed repository with regard to long-term waste isolation and short-term safety and retrievability objectives specified in the Code of Federal Regulations (1996), specifically 10 CFR 60.111, 60.112, and 60.122(c). Identification of such faults is also important to design criteria for the Geological Repository Operations Area (GROA) which require design of structures, systems, and components so that anticipated natural phenomena (e.g., vibratory ground motion or direct repository rupture due to seismic slip on active faults) will not interfere with the necessary safety functions [10 CFR 60.131(b) (1) (Code of Federal Regulations, 1996)]. The three main results documented in this report are:

- The development of a database of Type I faults, as defined in NUREG-1451 (McConnell et al., 1992). This database will serve as an input to seismic hazard analyses and interpretations, as well as for review and analysis of U.S. Department of Energy (DOE) documents on faulting and seismic hazard analysis.

- The assessment of the potential for slip on faults using slip tendency analysis (Morris et al., 1996; Ferrill et al., 1996b).

- The assessment of the potential for faulting and seismic hazards in light of fault length-displacement scaling relationships and alternative conceptual seismo-tectonic models of the YMR.

Fault Classification

Previous analysis (McKague, 1996) categorized 56 of the more than 400 YMR faults as Type II faults (those that are candidates for additional detailed investigations). Only faults included in the fault coverages of Nakata et al. (1982), Simonds et al. (1995), and Piety (1996) were considered in the fault classification study. The remaining faults were classified in McKague (1996) as Type III faults (those that will not affect repository performance or design). Of the 56 Type II faults, 52 are categorized as Type I in this report. Discriminating characteristics of Type I faults are (i) fault displacement(s) in the Quaternary,

[1]Key Technical Issue Implementation Plan for FY96. Nuclear Regulatory Commission. Washington, D.C.

(ii) favorable orientation of the fault planes for future slip assuming persistence of the modern (*in situ*) stress field, and (iii) a structural relationship with other Type I faults (McConnell et al., 1992). In addition, peak acceleration values equal to or exceeding 0.1 g were used as an additional discriminator of Type I faults for faults outside the controlled area. Peak acceleration values were generated using scaling relationships proposed in Wells and Coppersmith (1994) and Campbell (1987). Twelve attenuation functions for peak acceleration were reviewed. Peak accelerations calculated with Campbell's 1987 model generally yielded the largest accelerations for a given earthquake. For this reason, Campbell's model was used in evaluating ground motion associated with faults in this study.

Of the 52 Type I faults, the 24 that are capable of generating the largest peak accelerations at the site all lie within a 10-km radius of YM. Important faults more distant from the repository include the Bare Mountain (BM), Stagecoach Road (SCR), and Rock Valley (RV) faults, all of which are capable of generating peak accelerations at YM of greater than 0.25 g. No faults outside a 100-km radius of YM are capable of generating significant ($\geq$ 0.1 g) accelerations.

Despite having surface areas capable of producing peak accelerations greater than 0.1 g at YM, the Pagany Wash (PW), Sever Wash (SW), and Yucca Wash (YWF) faults lack significant evidence of Quaternary slip and have unfavorable orientations for slip in the current stress field, indicating that these faults are probably inactive. Therefore we classify them as Type III. Because of differing opinions as to its origin the Beatty Scarp (BS) is the only remaining Type II fault (c.f., Nakata et al., 1982; Simonds et al., 1995; and Piety, 1996).

The classification of faults presented in this study should not be considered static or immutable. It is anticipated that most of the faults classified as Type I in this study will remain Type I faults throughout the licensing process. However, new data could result in reclassification of some of these faults as Type II or Type III faults. Also with additional geologic or geophysical data or with the refinement of conceptual models, faults now considered Type III (i.e., faults that are neither Type I nor Type II), or faults that are currently unknown or hidden, could be classified as Type I faults. In addition, if the repository boundaries are changed, all faults incorporated within the new boundaries should be re-examined.

Slip Tendency

Review of slip tendency for the YMR shows that nearly all faults at YM have relatively high slip tendency values in the current (*in situ*) stress field except the northwest trending PWF, SW, and YWF faults. Moreover, because the maximum and intermediate principal stresses have nearly equal magnitudes, both strike-slip and dip-slip normal faults are expected to occur simultaneously. Given this stress state, a normal dip-slip mainshock could produce strike-slip aftershocks and strike-slip mainshocks could trigger normal dip-slip aftershocks (Ferrill et al., 1996b; Morris et al., 1996). Analysis of fault-plane solutions from the 1992 Little Skull Mountain earthquake sequence (centered ~15 km southeast of the proposed repository site at YM) confirms this expected pattern. The normal dip-slip M_s=5.6 Little Skull Mountain mainshock produced both normal dip-slip aftershocks on northwest and southeast dipping faults and right-lateral strike-slip aftershocks on north trending sub-vertical faults. Both aftershock populations cluster in orientation near the maximum slip tendency in the contemporary stress field.

In addition, slip tendency analysis was performed on alternative cross sections drawn across Crater Flat from Bare Mountain to Jackass Flat to test the effect of detachment depth and deformation style on the potential for seismic hazard at YM. Active faults that penetrate the entire thickness of the brittle crust pose the most significant potential seismic hazard because larger areas of the fault planes are favorably

oriented for slip. In contrast, faults that intersect a detachment within the brittle crust (e.g., at ~7 km depth) or in which deformation is greatest at the surface and diminishes with depth, limit the potential seismic hazard, because significantly smaller fault-surface areas are favorably oriented for future slip.

Additional Considerations from Fault Length-Displacement Scaling Relationships and Alternative Conceptual Tectonic Models

A linear power-law scaling relationship of fault-trace length versus cumulative vertical displacement (throw) was used to detect those dip-slip faults in the YMR which may have inaccurately reported fault lengths or displacements. Most faults in the YMR fall within the expected range established from fault data sets worldwide. However, the mapped fault-trace length of the BM appears too short for its cumulative throw. This observation coupled with recent structural and geophysical observations (Ferrill et al., 1996a; Connor et al., 1996) suggests that the BM probably extends well south of its presently mapped terminus in southern Crater Flat and is most likely hidden under the Amargosa Desert alluvium. Thus, a longer BM needs to be considered in future seismic hazard analyses. In contrast, both the Windy Wash (WW) and Ghost Dance (GD) faults appear too long for their accumulated throws. This observation suggests that either the offset estimates under-represent actual displacement or these faults are actually composed of a series of smaller distinct fault segments. If the latter is correct, then maximum moment magnitudes and peak accelerations estimated from these faults may be overestimated.

Two recently proposed tectonic models of the YMR suggest the presence of several significant blind seismic sources. In the Amargosa Shear model of Schweikert (1989), a buried (blind) strike-slip fault is proposed somewhere beneath Crater Flat. This fault would be a first-order crustal strike-slip fault similar to the Death Valley-Furnace Creek fault and, as such, would have the potential for a M_w=7.8 earthquake. This magnitude earthquake 8 km from the repository (halfway between YM and BM) would produce a peak acceleration at the proposed repository of 0.76 g. Similarly, in the pull-apart models of Fridrich (1996), several cross-basin strike-slip faults are proposed (including an active Yucca Wash Fault) with the potential of M_w=6.6 to M_w=6.8 and peak accelerations between 0.65 and 0.74 g at the proposed repository.

Given the seismic potential of these inferred faults, future refinement of the conceptual tectonic models of the YMR, as well as better characterization of blind seismic sources, is required to fully appraise their effects on repository safety and performance. Recent apatite fission-track ages from BM and the Striped Hills (Ferrill et al., 1996b) do not support Schweikert's (1989) reconstruction, calling into question the existence of the Amargosa Shear. The pull-apart model of Fridrich (1996) is more tenable (Stamatakos and Ferrill, 1996), although a more direct observation of basin-bounding and cross-basin strike-slip faults is needed to authenticate this interpretation.

1 INTRODUCTION

1.1 BACKGROUND

The Nuclear Regulatory Commission (NRC) developed NUREG-1451, Staff Technical Position on Investigations to Identify Fault Displacement Hazards and Seismic Hazards at a Geologic Repository (McConnell et al., 1992) to provide guidance to the U.S. Department of Energy (DOE) on appropriate investigations for identification of fault displacement hazards and seismic hazards at a generic geologic repository. In the present report, guidance from McConnell et al. (1992) is used to classify faults previously identified in McKague (1996) as Type II faults (candidates for additional detailed investigations), as Type I faults (those that could affect the repository design or performance), or Type III faults (those that will not affect repository design or performance).

1.2 SCOPE

In McKague (1996), three coverages (Nakata et al., 1982 - electronic coverages; Simonds et al., 1995 - electronic coverage; and Piety, 1996 - textural coverage) were used to classify more than 400 faults within a 100-km radius of the proposed Yucca Mountain (YM) repository site. Earthquakes and fault displacements on most of the faults will have no affect on the proposed repository design or performance because they are too far from the repository or too small to generate significant ground motion at YM, or both. Broad screening criteria were used to assess the three fault coverages in order to identify faults important to repository design or performance. The faults in the coverages were tested quantitatively against the criteria. Faults identified using the criteria of McConnell et al. (1992) as having the potential for little or no effect on the repository were treated as Type III and not considered further. The remaining 56 faults required additional characterization or closer study to determine their potential effects on design and performance.

This study reviews the faults in the remaining group individually in light of available information to determine if these 56 faults meet the criteria to be classified as Type I faults according to NUREG-1451. Only potential ground motion or fault displacement hazards were considered in this study. Other disruptive conditions related to structural deformation, such as changes in rock properties and the effects of structural deformation on water and magma flow, were not considered.

The principal outcome of this study is to provide a basis for the NRC to review the DOE determination of significant faults. With this information, the NRC may be able to clarify or resolve technical concerns related to structural deformation and seismic hazards at the proposed repository by identifying faults for which additional information is required, and eliminate from further consideration those faults which will have little or no effect on repository design or performance.

In this report the term "fault" is as proposed by Groshong (1988): "a tabular region across which the displacement parallel to the zone is appreciably greater than the width of the zone and in which the deformation is greater than outside the zone." Many of the faults shown in Figures 1-1 and 1-2 as single fault traces actually occur as two or more closely associated fault surfaces.

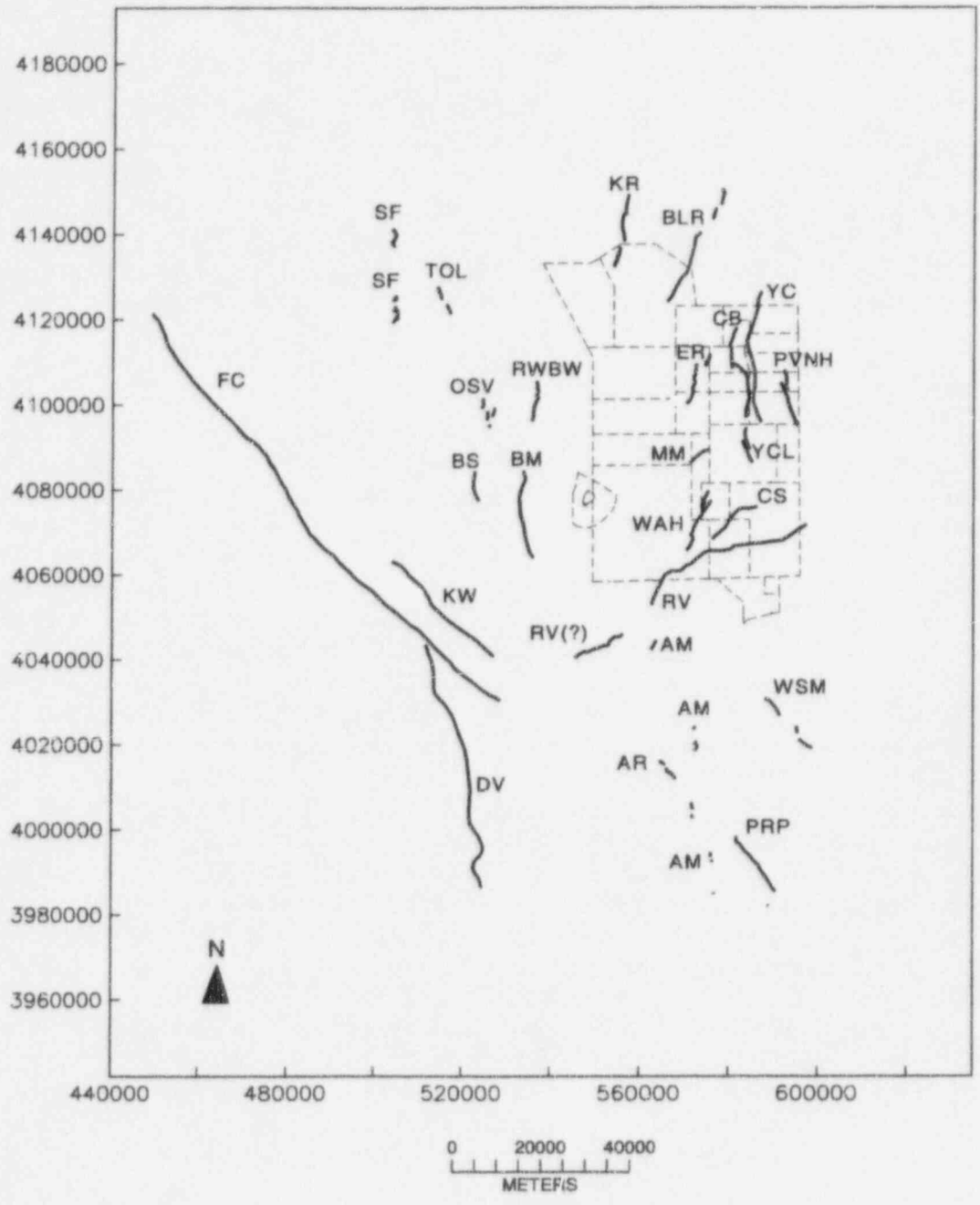

Figure 1-1. Regional map showing locations of faults beyond a 10 km radius but within a 100-km radius of Yucca Mountain that were identified as Type II faults in McKague (1996). Locations of these faults are from Nakata et al. (1982); Sawyer et al. (1995); and Piety, (1996). Fault names are given in Appendix B. The fault labeled RV(?) is considered part of the Rock Valley fault system in this study. The Nevada Test Site, the proposed repository boundary, and the repository controlled area are shown by dashed lines. All faults shown are Type I, except fault labled BS. Map coordinates are Universal Transverse Mercator (UTM) Zone 11.

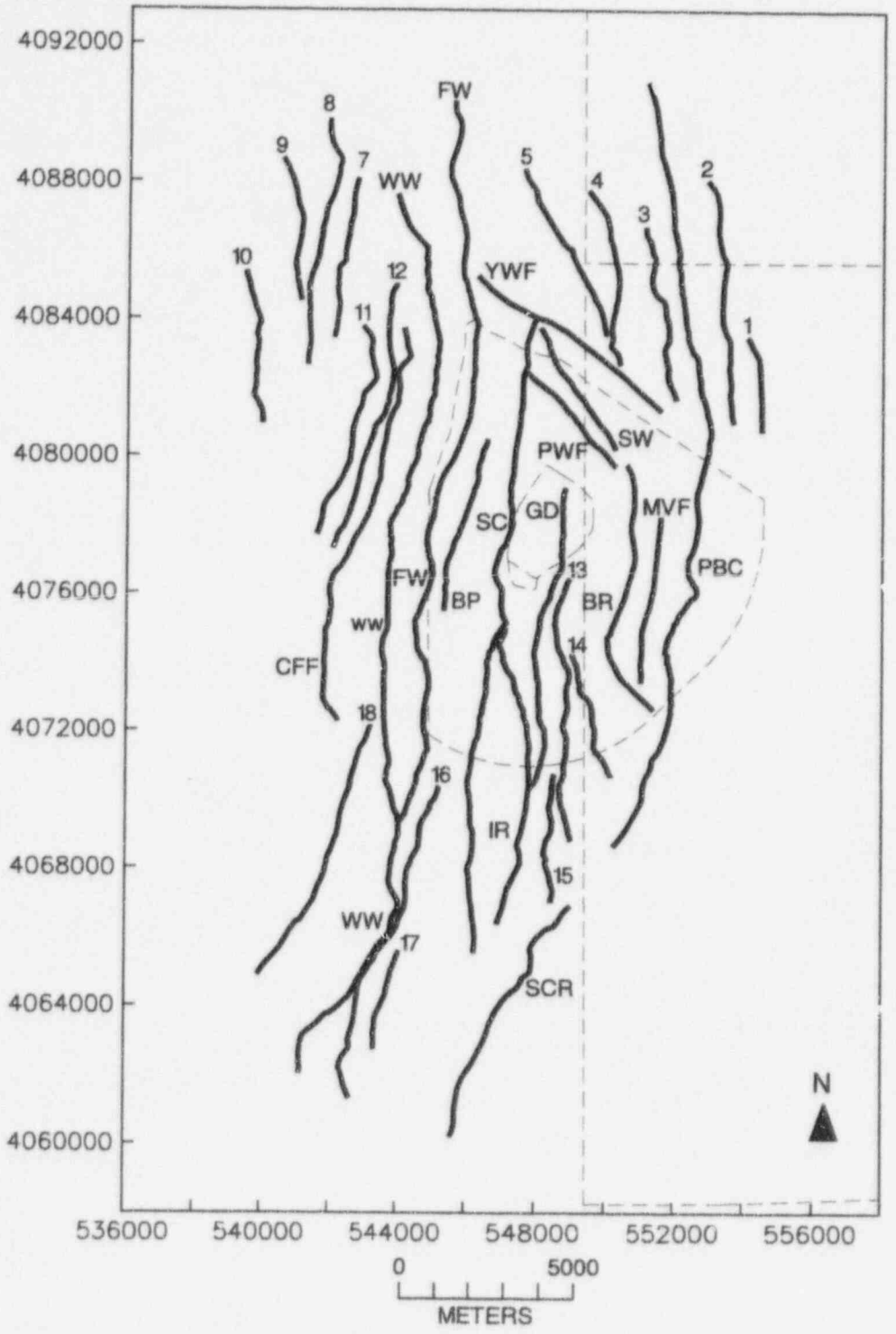

Figure 1-2. Locations of faults at or near Yucca Mountain from Simonds et al. (1995) and Frizzell and Shulters (1990). Repository boundary, controlled area boundary, and Nevada Test Site boundary are shown by dashed lines. All faults are Type I except those labled PWF, SW and YWF. Map coordinates are Universal Transverse Mercator (UTM) Zone 11.

2 CLASSIFICATION OF FAULTS

2.1 FAULT CLASSIFICATION APPROACH

NUREG-1451 developed a classification of faults according to their potential to affect repository design or performance. The classification and d ·inguishing criteria are given in Table 2-1. The classified faults in this study include faults from the coverages of Nakata et al. (1982), Simonds et al. (1995), and Piety, (1996). All faults in these coverages are known or assumed to be Quaternary or younger. Many faults within 100 km of the potential repository were not included or considered in this study. These include faults within 100 km of YM where there is little or no evidence of the age of last movement (i.e., faults within the Paleozoic inliers of Bare Mountain and Calico Hills and the resurgent dome of Timber Mountain). We also did not consider faults less than 4 km long, because earthquakes generated by movement along such faults would be quite small, less than $M_w < 5.6$. This study does not include pre-Quaternary faults that could be reactivated in the future or blind faults that are assumed to be present in various conceptual models. The potential impacts of various conceptual models on seismic hazard assessments are discussed in Section 4.2.

To summarize the criteria detailed in Table 2-1, Type I faults are those faults that must be characterized by detailed geologic investigation because their (i) age of displacement, (ii) location with respect to the repository, (iii) length, (iv) orientation, or (v) historic seismicity indicates a potential to affect repository design or performance. Type I faults include faults within the controlled area that have demonstrable Quaternary (<2.0 m.y.) displacement. Outside the controlled area, Type I faults must show evidence of Quaternary displacement and be of sufficient length or orientation to potentially affect the repository, or they must be seismically active, or have a direct (branching) relationship with a seismically active fault.

The previous study of McKague (1996) identified Type III faults—those that will not affect repository design or performance. Type III faults include faults that (i) are located outside the faulting component (the region of consideration, 100 km); (ii) are located within the faulting component but of insufficient length or at locations or with orientations that would not affect repository design or performance; (iii) experienced most recent displacement prior to the Quaternary; (iv) are unfavorably oriented in the current stress field for displacement; or (v) are demonstrably seismically inactive. In the previous study of McKague (1996) 56 faults in the Yucca Mountain region (YMR) were classified as Type II; the remaining faults were classified as Type III faults.

Type II faults require additional characterization to determine if their location, length, orientation, age of displacement, and seismicity have a potential effect on repository design or performance. Faults classified as Type II require additional investigations to determine if they should subsequently be reclassified Type I or Type III faults for design and performance assessment. In this report, information on the age of the faults and the resultant ground motion from a maximum magnitude earthquake are reviewed.

2.2 DATA SOURCES

To classify faults according to the system described in NUREG-1451, Quaternary faults from three individual fault coverages were assessed. Electronic coverage, out to 100 km, was provided by the maps of Nakata et al. (1982). In order to show the location of all faults considered, 11 faults from

Table 2-1. Description of fault types and criteria for classification based on NUREG-1451 (McConnell et al., 1992)

Fault Type	Criteria
Type I - Faults that could affect repository design or performance and must be characterized to determine consequence of displacement.	1. Faults within the controlled area[1] that are or could be subject to displacement as demonstrated by evidence of Quaternary displacement (< 2.0 m.y.). 2. Quaternary faults outside the controlled area, but within the faulting component,[2] and of sufficient length and location that they may affect repository design and performance. 3. Faults that are favorably oriented in the current stress field for fault displacement, are seismically active, or have a direct relationship with an active fault.
Type II - Faults with a high degree of uncertainty about possible effects on the repository. Further studies or characterization are needed to determine if faults meet Type I criteria.	1. Faults outside the controlled area but within the faulting component that are of sufficient length and located such that they may affect repository design and performance. 2. Faults that show evidence of displacement in the last 2 m.y.
Type III - Faults that will not, based on current information, affect repository design or performance.	1. Faults that are outside the faulting component. 2. Faults located within the faulting component of insufficient length and orientation such that displacement along them could not affect repository design or performance. 3. Faults whose most recent displacement is demonstratably older than the Quaternary. 4. Faults that are unfavorably oriented in the current stress field for fault displacement. 5. Faults that are demonstrably seismically inactive.

(1) Controlled area means a surface location, to be marked by suitable monuments, extending horizontally no more than 10 km in any direction from the outer boundary of the underground facility (see Figures 1-1 and 1-2).
(2) Faulting component means that portion of the earth's crust that needs to be investigated to encompass those faults that might have an effect on repository design and performance or provide significant input into models used to assess repository performance resulting from fault displacement.

Sawyer et al. (1995) and two faults from Piety (1996) were added to those in the electronic coverage of Nakata et al. (1982) shown in Figure 1-1. Two faults, Amargosa River (AR) and Ash Meadows (AM), were digitized from the map of Piety (1996) as they were not available in the electronic coverages (Figure 1-1). The Nakata et al. (1982) coverage is at a scale of 1:2,500,000 and provides coverage for both the Basin and Range and the Rio Grande Rift provinces (Martin, 1995). The maps of Sawyer et al. (1995) and Piety (1996) are at a scale of 1:100,000. Some geological interpretation of the electronic map was done to link segments of faults in order to maximize their length and thus their potential to be classified as Type I or II faults. For example, short segments in the Nakata et al. (1982) coverages of the Rock Valley (RV) fault were linked together as a single segment with a total length of 65 km. This approach assures that a more conservative fault coverage was used in this first phase of analysis.

Local map coverage around YM was from Simonds et al. (1995) at a scale of 1:24,000. This provides local coverage roughly within 14 km of the repository (Figure 1-2). Extensions of several faults to the north and the Stagecoach Road (SCR) fault to the south that extended beyond the coverage were added from a digitized version of the faults in the Center for Nuclear Waste Regulatory Analyses (CNWRA) Geographical Information System (GIS) database (Martin, 1995). This coverage was also in electronic format.

2.3 RESULTS OF EARLIER STUDY

Two digital map coverages in the CNWRA electronic GIS database and one textual coverage of Quaternary faults within 100 km of YM were analyzed in order to identify and screen Type III faults in the YMR (McKague, 1996). In that study all faults < 4 km long were eliminated from consideration. The most effective screening criteria of the remaining faults were peak horizontal acceleration and slip tendency. Other generic criteria recommended in NUREG-1451, such as age of last displacement and historic seismicity, were ineffective in screening the fault population in the YMR. All faults in the three coverages were considered by their authors to have Quaternary displacement. The YMR historic seismicity is a limited discriminator in fault classification because the historic seismic record is brief (Ferrill et al., 1995; 1996b) and the modern seismic activity is commonly minimal, diffuse, and difficult to relate to the subsurface geology.

2.4 ATTENUATION FUNCTIONS

A deterministic assessment of the potential influence of seismicity on preclosure safety and design or long-term performance hinges on knowledge of anticipated peak ground accelerations at the repository site generated from earthquakes in the surrounding region. Estimates of peak acceleration for this assessment are derived from empirical attenuation functions (based on strong motion records) that describe ground motions in terms of the largest possible earthquake a given fault can generate (maximum magnitude earthquake) and closest approach of the fault to the site. Distance to the site is easily determined from geologic maps. Maximum magnitudes are derived from empirical relationships that match historic earthquakes with their corresponding surface ruptures measured along active faults (e.g., Wells and Coppersmith, 1994).

At least twelve attenuation functions for seismic wave accelerations have been published between 1981 and 1993 (Joyner and Boore, 1981; Campbell, 1981; Sadigh et al., 1986; Campbell, 1987; Sabetta and Pugliese, 1987; Joyner and Boore, 1988; Abrahamson and Litehiser, 1989; Campbell, 1989; Tsai et al., 1990; Idriss, 1991; Campbell, 1993; Boore et al., 1993). For small source-to-site distances

(~10 km or less) and magnitudes larger than 6.0, Campbell (1987), Sadigh et al. (1986), and Tsai et al. (1990) yield the largest peak accelerations (Figure 2-1). For distances greater than 10 km all 12 functions yield similar values (within a range of approximately 0.2 g) (Figure 2-1). Because Campbell (1987) generally predicts the largest ground motions for a given earthquake, it was deemed most appropriate (most conservative) for discrimination of Type I faults.

Peak accelerations were also calculated for all 1,418 faults in the electronic coverages of Simonds et al. (1995) and Nakata et al.(1982) using the attenuation models of Tsai et al. (1990) and Campbell (1987) (Figure 2-2). These results indicate that no faults greater than approximately 100 km from the YM site are capable of generating peak accelerations greater than 0.1 g. Given the 0.1 g cutoff (McConnell et al., 1992), we therefore define the faulting component as the area within a 100 km radius of YM.

2.5 DISCUSSION

Of the 56 Type II faults from the previous study, 52 faults have been identified as Type I faults (Appendix A). All Type I faults in the YMR cut or offset Quaternary alluvium or colluvium and have estimated peak accelerations equal to or greater than 0.10 g as proposed by McConnell et al. (1992). The magnitude (M_w) of an earthquake is calculated from the maximum length (L) of the fault using the equation from Wells and Coppersmith (1994):

$$M_w = 5.08 + 1.16 \times \log L, \tag{2-1}$$

Acceleration is calculated using the attenuation formula of Campbell (1987):

$$\ln(A) = -2.893 + (0.85M_w) - 1.25\ln((r^2+16)^{1/2} + 0.0872e^{0.678M_w}) - 0.0059r \tag{2-2}$$

where A is average acceleration and r is the closest approach of the fault to the center of the repository at the surface. Peak acceleration (A_p) is calculated using the following equation:

$$A_p = 1.12 \cdot A \tag{2-3}$$

Insufficient information exists for the Beatty Scarp (BS) fault to allow its classification as either a Type I or Type III fault. There are differences of opinion as to the origin of the scarp. Cornwall and Kleinhampl (1961) consider the BS to be a fault scarp, whereas Swadley et al. (1988) and Anderson and Klinger (1996) consider it to be a remnant of erosion of alluvial fans originating on the southwest flank of Bare Mountain by the Amargosa River. Based on seismic data, Harding (1988) also concluded BS is not a fault.

Three northwest-trending faults, the Pagany Wash (PWF) fault, the Sever Wash (SW) fault, and the Yucca Wash (YWF) fault, are classified as Type III faults. This is based on weak to absent evidence of Quaternary displacement (Simonds et al., 1995, Dickerson, 1996) in combination with their orientations in the current regional stress field. Slip tendency analysis supports the interpretation derived from field mapping and surface geophysical surveys indicating these faults are much less likely to move than the more N- and NE-trending faults. With the large number of faults in the YMR favorably oriented for slip, it is unlikely that slip would occur along three relatively short faults oriented at a high angle to the regional maximum horizontal stress. Furthermore, because the stress field has rotated clockwise

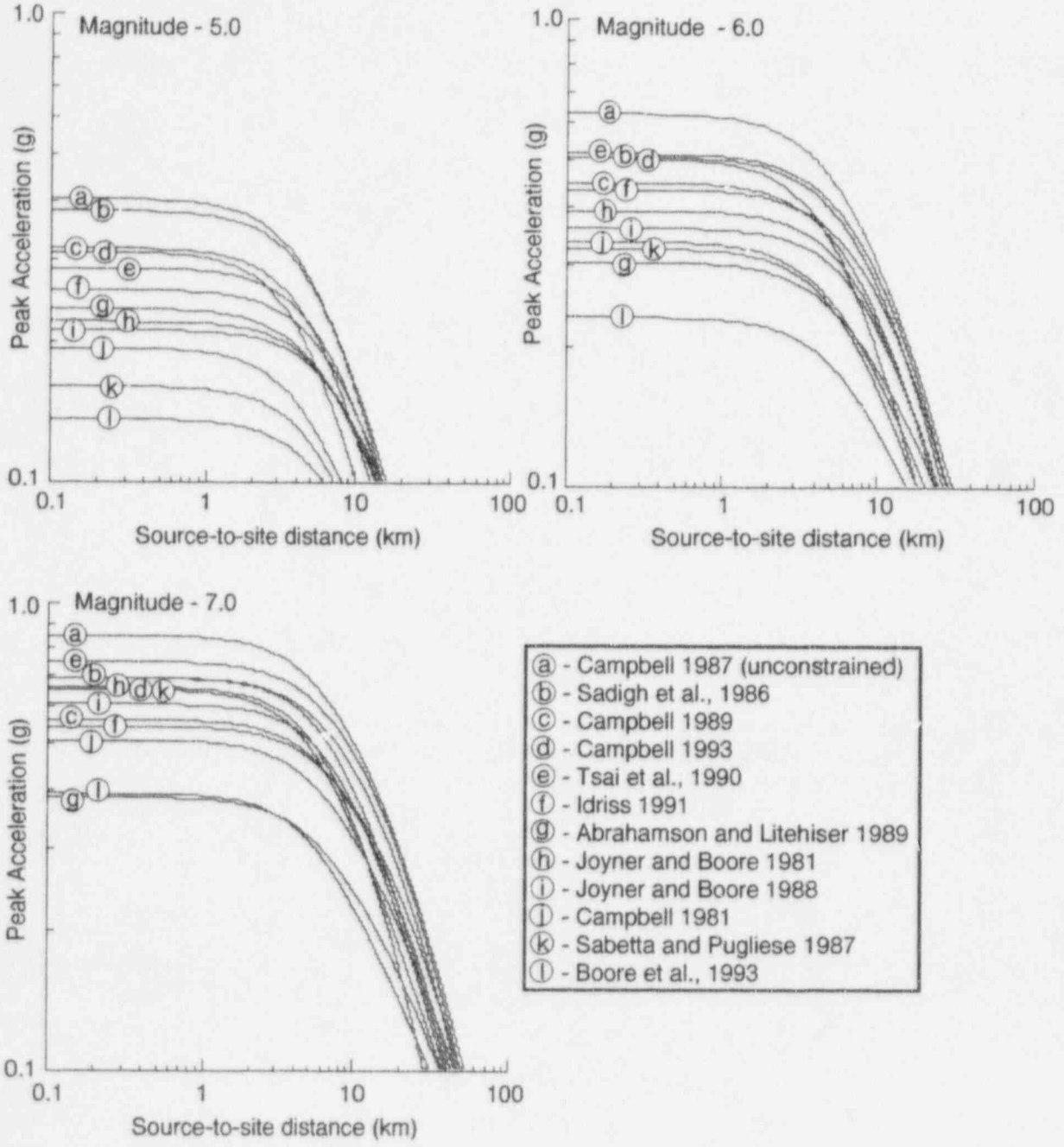

Figure 2-1. Peak horizontal acceleration plotted as a function of site-to-source distance for 12 previously published attenuation functions. Three plots show attenuation models for magnitude 5.0, 6.0, and 7.0 earthquakes.

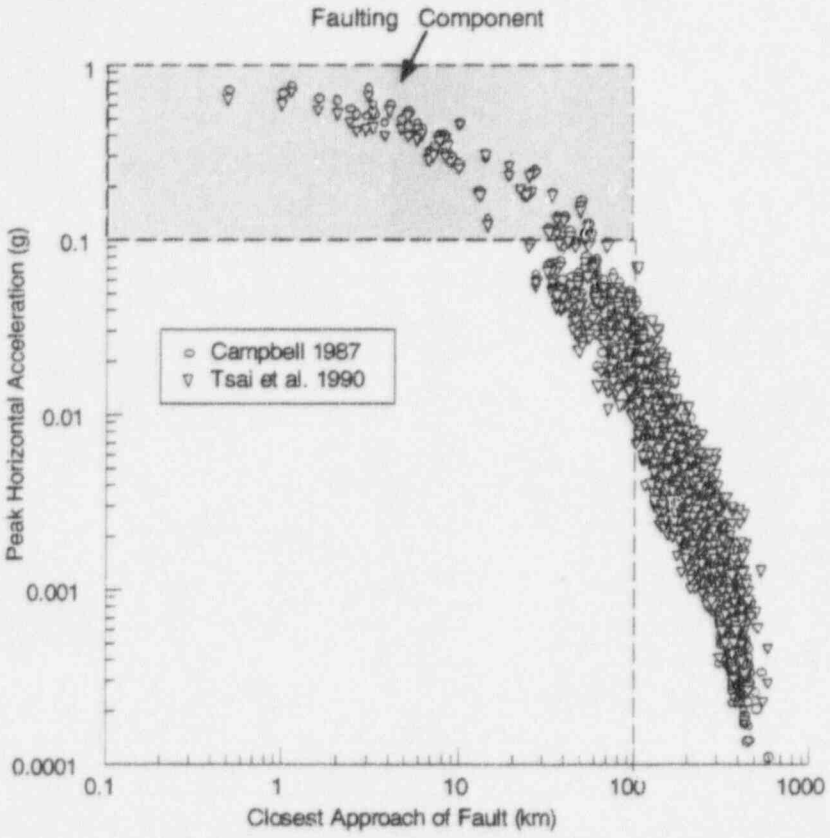

Figure 2-2. Peak horizontal acceleration for the 1,418 faults within a 700-km radius of the Yucca Mountain site assuming the maximum magnitude earthquake for each fault. Maximum magnitudes for each fault were derived from Wells and Coppersmith (1994). Dashed line shows the 0.1 g cutoff.

through the Neogene (Zoback et al., 1981), the probability of slip on NW-trending faults in the next several m.y. may be decreasing. If the maximum horizontal stress rotated clockwise from its present day orientation of about N28E to a more northeast orientation, it would become perpendicular to these NW-striking faults, which range in average strike from N35 - 55°W, causing a further decrease in slip tendency of NW-trending faults. Faults in the YMR are further evaluated using slip tendency analysis in Section 3.4.

The Drill Hole Wash fault is also a NW trending fault. However, because it is less than 4 km long it did not meet the criteria used in McKague (1996) to identify Type II faults, i.e., length greater than 5 km. Therefore, it is not considered in this study. Because of its orientation and lack of definitive Quaternary offset it would be considered a Type III fault, if it were included in this study.

3 SLIP TENDENCY OF FAULTS IN THE YUCCA MOUNTAIN REGION

The pattern of faults in the YMR is the result of progressive deformation. Although the earth's crust in the YMR accumulated faults related to several episodes of deformation continuing to the present, many of the existing faults are no longer likely to slip. The potential for slip on a fault is largely a function of the contemporary stress state, frictional and strength characteristics of the fault, and fault geometry and orientation. Although frictional and strength characteristics of a fault play a role in determining which favorably oriented fault will actually slip, these characteristics play a relatively small role in determining which faults in a set of variably oriented faults have a tendency to slip within a given stress state.

3.1 DEFINITION OF SLIP TENDENCY

Slip is likely to occur on a fault surface when the resolved shear stress, τ, on that surface equals or exceeds the frictional resistance to sliding, F, which is proportional to the normal stress, σ_n, acting across that surface (Jaeger and Cook, 1979). Whether or not a surface will actually slip depends upon its cohesive strength, if any, and the coefficient of static friction, μ. For a cohesionless fault at the instant of sliding

$$F \leq \tau = \mu \sigma_n \tag{3-1}$$

and

$$\mu = \tau / \sigma_n \tag{3-2}$$

The slip tendency, (T_s), of a surface is defined as the ratio of shear stress to normal stress acting on that surface (Ferrill et al., 1994, 1995, 1996b; and Morris et al., 1996)

$$T_s = \tau / \sigma_n \tag{3-3}$$

and, as such, depends solely on the stress field (stress tensor) and the orientation of the surface. The coefficient of static friction, μ, is the value of T_s that will cause slip on a cohesionless surface; often referred to as the fault "strength" in analysis of earthquake focal mechanisms. The implication of fault strength is that, if slip occurs on a surface with a low slip tendency, the fault must have a low μ and thus is "weak."

3.2 STRESS FIELD AT YUCCA MOUNTAIN

YM is located in the southern Great Basin near the projected intersection of the Intermountain Seismic Belt and the Walker Lane Seismic Belt (summarized by Ferrill et al., 1996b). The Walker Lane Seismic Belt is characterized by both normal and strike-slip earthquake focal mechanisms. Based on Coulomb criteria for faulting, this pattern suggests that the maximum principal stress is alternatively horizontal (strike-slip faulting) and vertical (normal faulting). Furthermore, this pattern suggests that the maximum (σ_1) and intermediate (σ_2) principal stresses have similar magnitudes. More importantly, the least principal stress, (σ_3), is generally horizontal and trends WNW-ESE. Therefore, σ_3 is the unique

axis and has the most direct control on the pattern of fault slip tendency. Numerous authors have noted the apparent synchronicity of both normal and strike-slip faulting in the southern Great Basin (Wernicke et al., 1988; Wesnousky and Jones 1994). Some workers (Bellier and Zoback, 1995) have suggested that this apparent synchronicity of normal and strike slip faulting may actually be a function of relatively short-term "flip-flopping" of the maximum and intermediate principal stress between vertical and horizontal. In the following sections, we illustrate that it is not necessary to invoke a flip-flopping stress field for the YMR, based on contemporary stress measurements and the sequence of aftershocks following the 1992 Little Skull Mountain earthquake.

From extrapolations of measurements described by Stock et al. (1985) and Stock and Healy (1987) corrected for assumed hydrostatic pressure, Morris et al. (1996) estimated the following effective principal stresses at a depth of 5 km: σ_1 = vertical = 90 MPa, σ_2 = N25°E–N30°E = 45–65 MPa (50–72 percent of σ_1), and σ_3 = N60°W–N65°W = 20–29 MPa (22–32 percent of σ_1). Slip tendencies for faults in this stress field are greatest for moderately to steeply dipping faults with north-south to northeast-southwest strikes (Figure 3-1). These conclusions agree with those of Stock et al. (1985).

3.3 ASSESSMENT OF FAULT PLANE SOLUTIONS: THE LITTLE SKULL MOUNTAIN SEQUENCE

The M_s 5.4 Little Skull Mountain earthquake occurred about 15 km southeast of YM on June 29, 1992, the day after the M_s 7.6 Landers earthquake. Comparisons of the nodal planes for the Little Skull Mountain mainshock and 85 aftershocks (Harmsen, 1994) show strong agreement between the pattern of slipped fault planes and those expected, based on slip tendency (Figure 3-2). As described by Harmsen (1994), the pattern of slipped faults in the Little Skull Mountain earthquake sequence is dominated by dip slip on southeast-dipping normal faults and right-lateral strike slip on vertical north-south trending faults. This pattern is predicted by slip tendency analysis of the YM stress field (Figure 3-1) and confirms the interpretation that strike-slip and normal faults can simultaneously be active in the YM area. Moreover, the pattern shows that normal faults can trigger strike-slip aftershocks, and strike-slip mainshocks can potentially trigger normal aftershocks (Ferrill et al. 1994; Ferrill et al. 1996b; Morris et al. 1996).

3.4 SLIP TENDENCY ANALYSIS OF FAULTS IN THE YUCCA MOUNTAIN REGION

Slip tendency analysis of faults in the YMR and Nevada Test Site (NTS) region (compiled by Sawyer et al., 1995) was performed assuming a paleo-stress state (after Zoback et al., 1981) that may have formed many of the faults that cut Miocene volcanics in the region [Figure 3-3(a)]. The assumed stress values are those of Morris et al. (1996). In this paleo-stress state, σ_3 is modeled as east-west. Note that nearly all steeply dipping faults in the modeled stress state are in orientations of high slip tendency.

Slip tendency analysis of faults in the YMR and NTS region, assuming the contemporary stress field of the YMR [Figures 3-3(b), 3-4, and 3-5] as described by Morris et al. (1996), illustrates that most faults in the vicinity of YMR are in orientations of relatively high slip tendency.

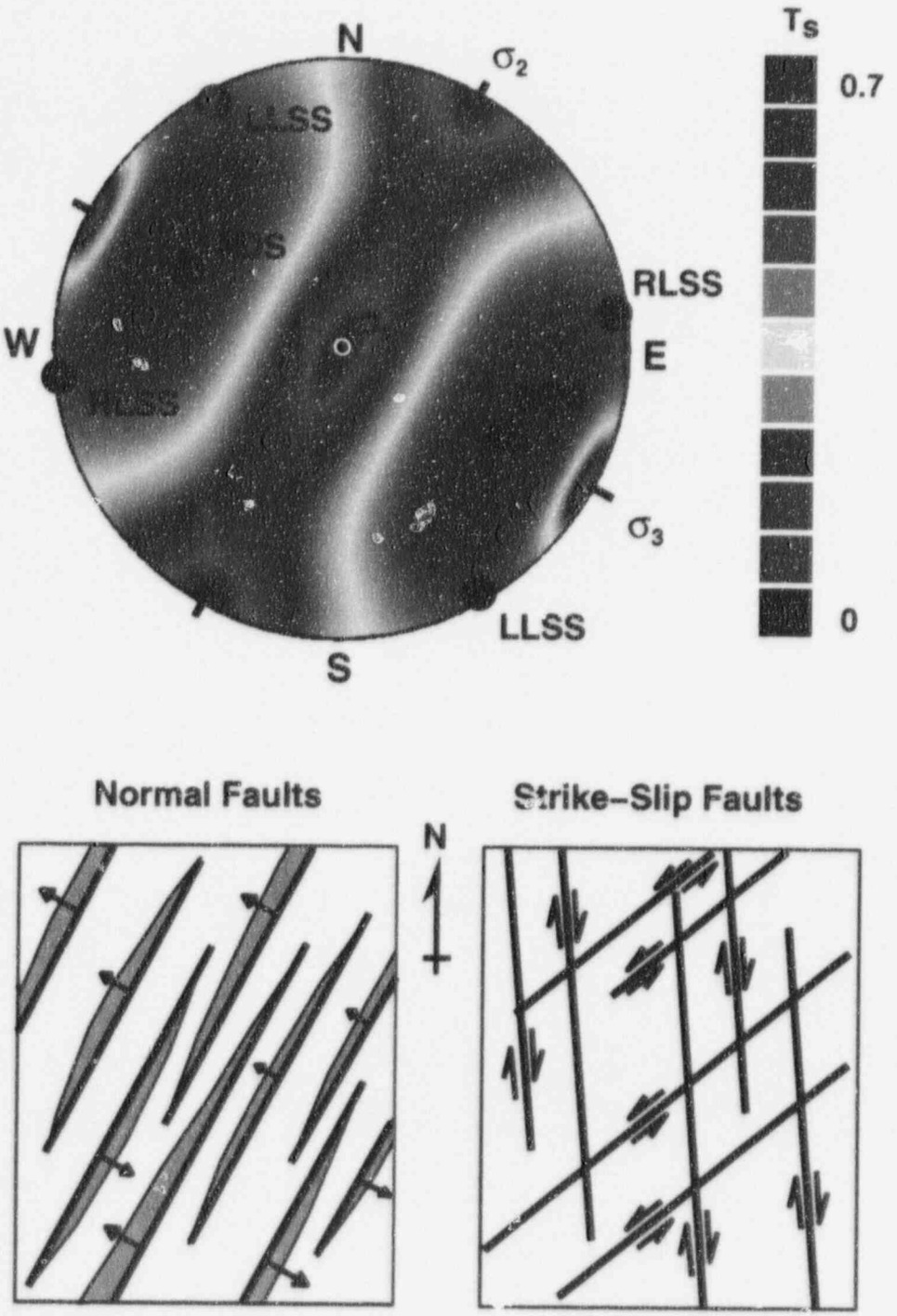

Figure 3–1. Slip tendency plot illustrating the fault plane orientations with greatest slip tendency and predicted slip vectors in the current stress field for Yucca Mountain, Nevada. Dots labelled RLSS, LLSS, and NDS represent poles to right–lateral strike slip, left–lateral strike slip, and normal dip slip faults respectively. Maps illustrate examples of normal and strike–slip faults that have high slip tendency in the current stress field. Arrows indicate expected slip directions on faults.

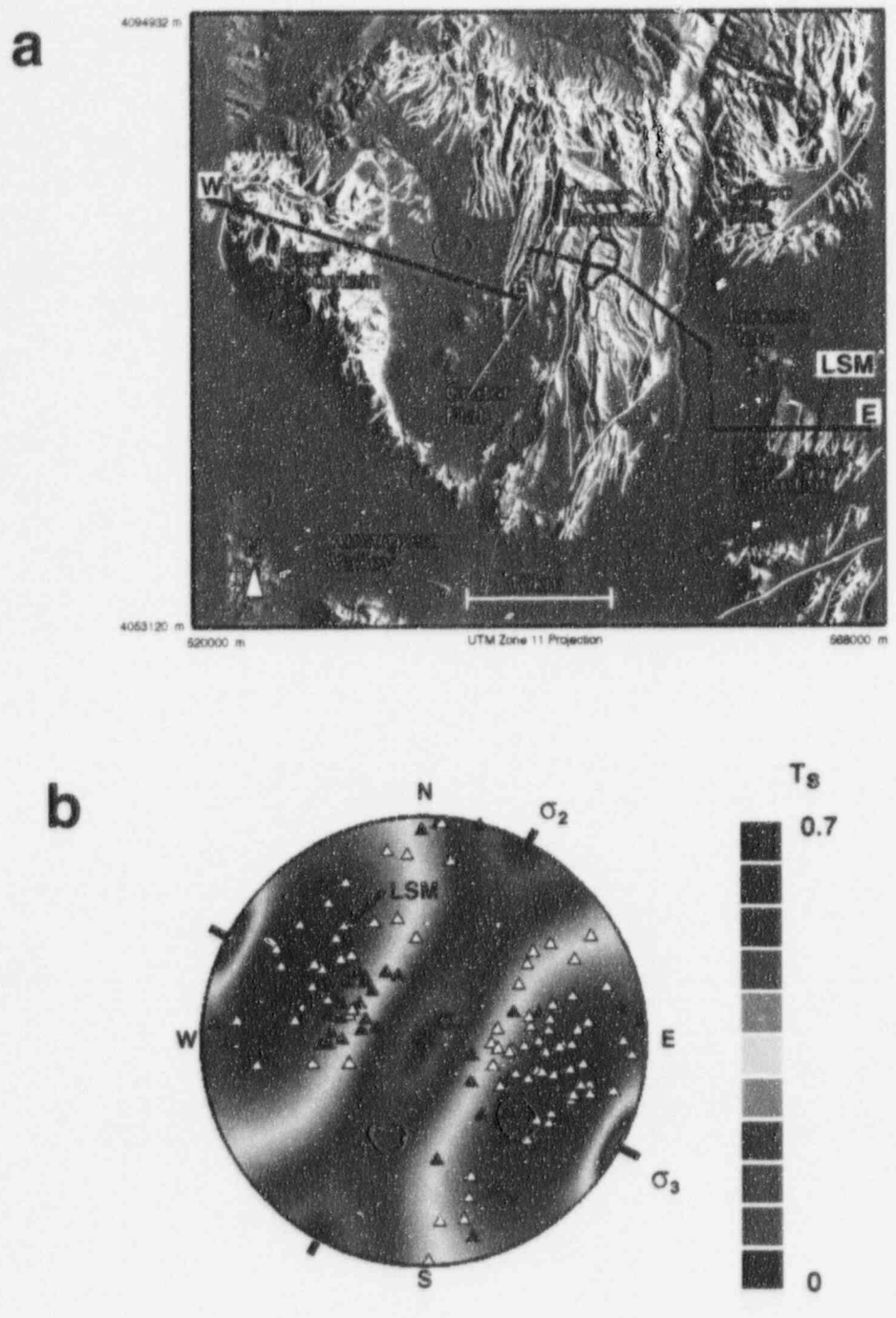

Figure 3–2. (a) Digital elevation model of Yucca Mountain area showing the location of the epicenter of Little Skull Mountain earthquake (LSM). (b) Slip tendency plot for Yucca Mountain overlaid with poles to nodal planes for Little Skull Mountain earthquake and aftershocks illustrates close agreement between actual slipped planes and orientations of predicted high slip tendency (yellow to red colors). White triangles are poles to selected nodal planes and black triangles are poles to alternate planes as chosen by Harmsen (1994).

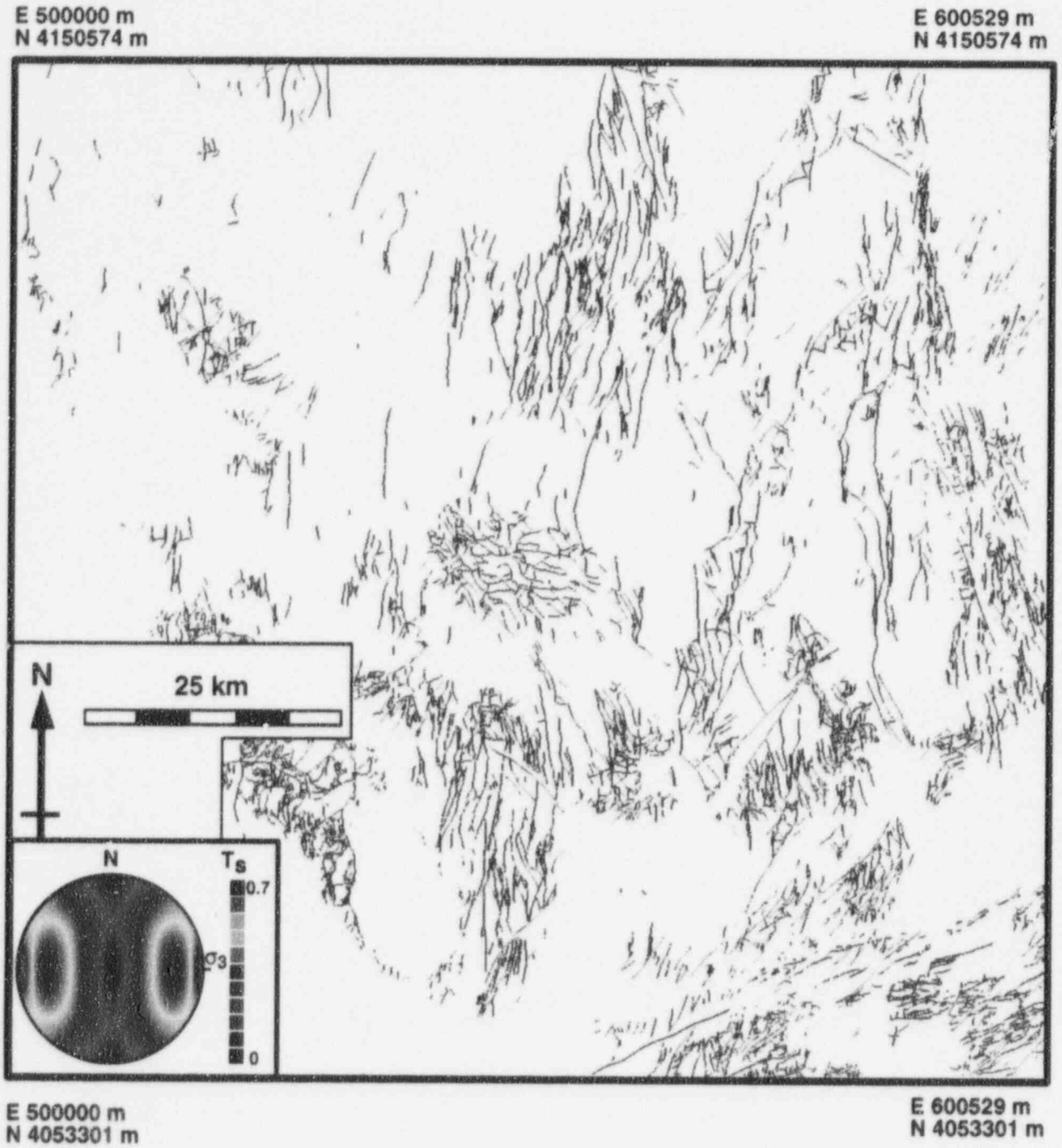

Figure 3–3. (a) Slip tendency analysis of faults in the Yucca Mountain and Nevada Test Site regions compiled from Sawyer et al. (1995) and Monsen et al. (1992) assuming an inferred paleo–stress state that may have formed many of the faults that cut Miocene tuffs in the region. The assumed stress values are those of Morris et al. (1996). σ_3 is modeled as east–west trending. Note that nearly all linear faults are in orientations of high slip tendency in the modeled stress state. East trending faults north of Yucca Mountain have low slip tendency with respect to the modeled stress state. These faults in the Timber Mountian caldera probably formed in a nearly uniaxial stress state dominated by a vertical σ_1.

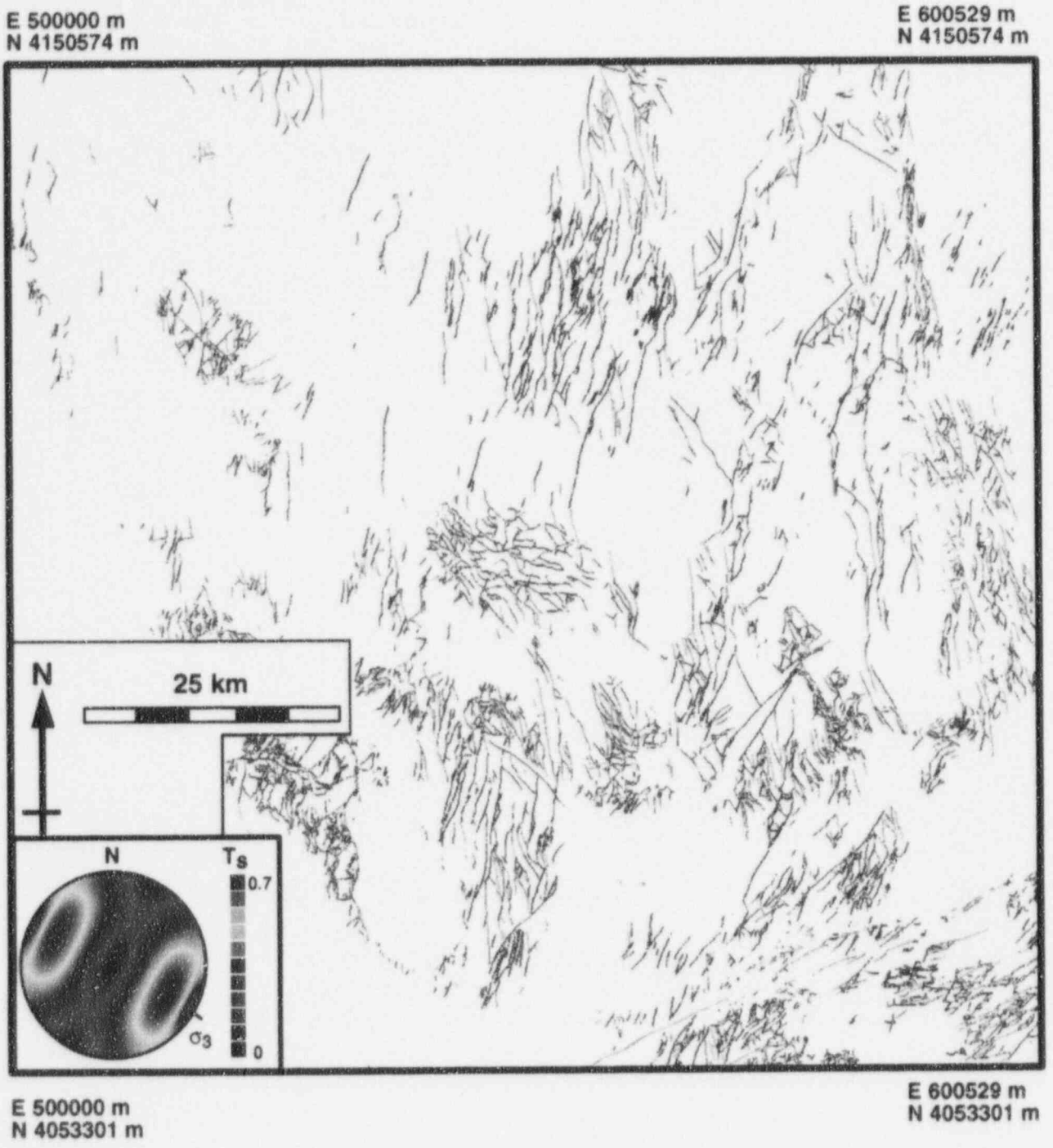

Figure 3–3. (b) Slip tendency analysis of faults in the Yucca Mountain and Nevada Test Site regions assuming stress field interpretation of Morris et al. (1996)

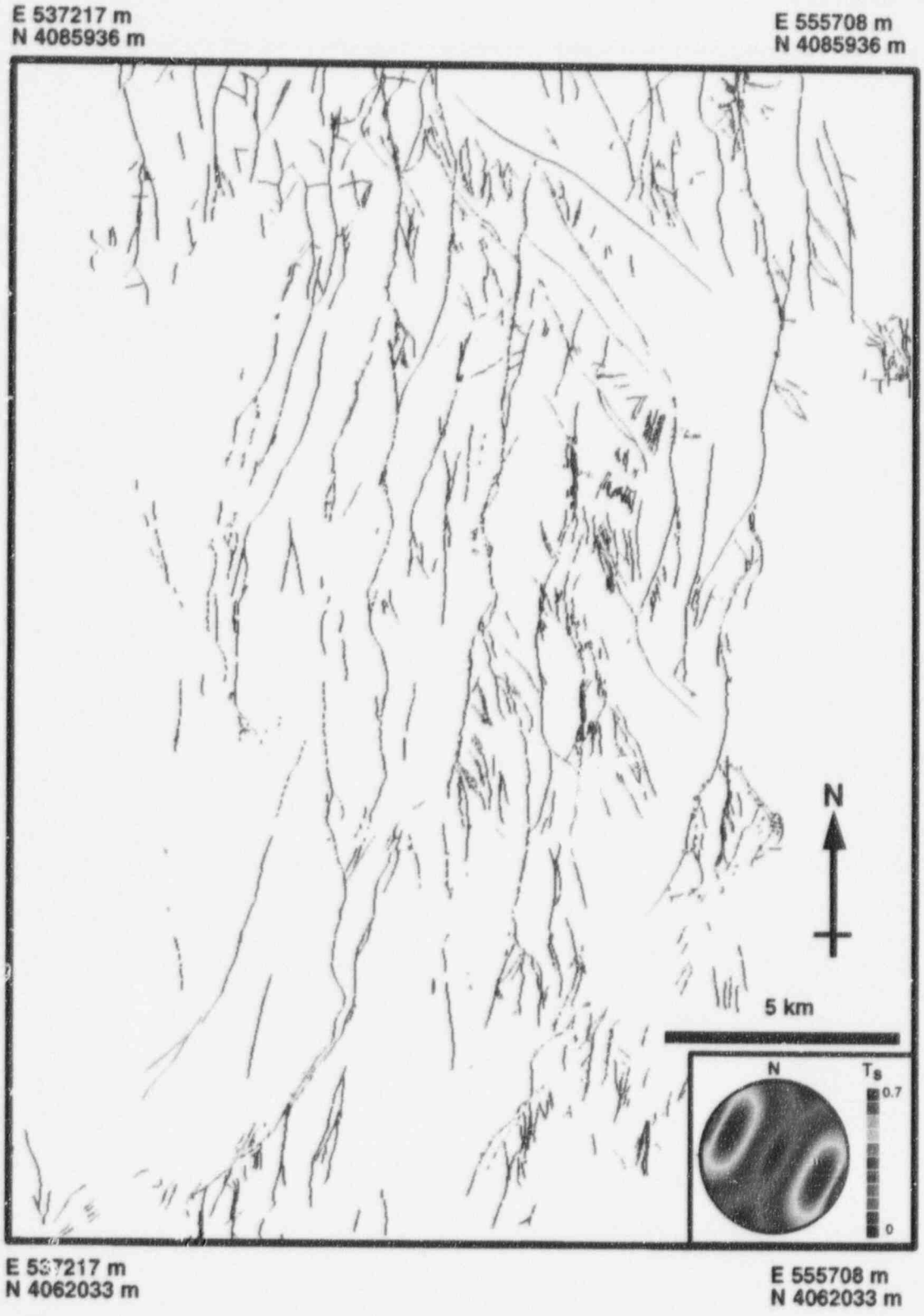

Figure 3–4. Slip tendency analysis of Yucca Mountain faults based on fault compilation of Simonds et al. (1995)

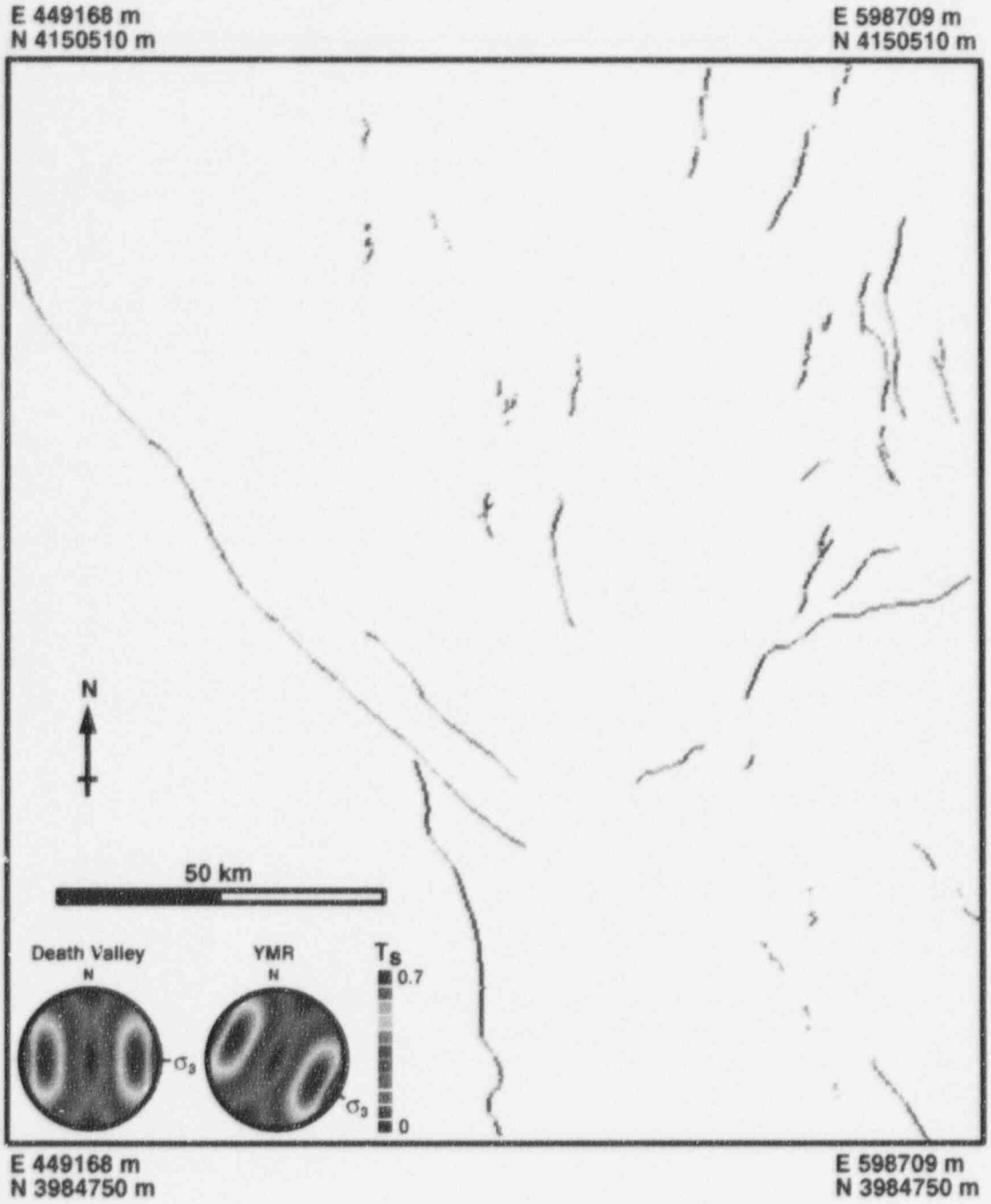

Figure 3–5. (a) Slip tendency analysis of faults shown in Figure 1–1. The FC fault (long NW–SE fault on the left half of the figure) has a low slip tendency in the modeled stress state appropriate for the YMR (with σ_3 trending WNW). However, as shown, its slip tendency is moderate to high when an alternate stress state dominated by E–W trending σ_3 which is more appropriate for the Death Valley–Owens Valley region is used (Zoback, et al. 1992).

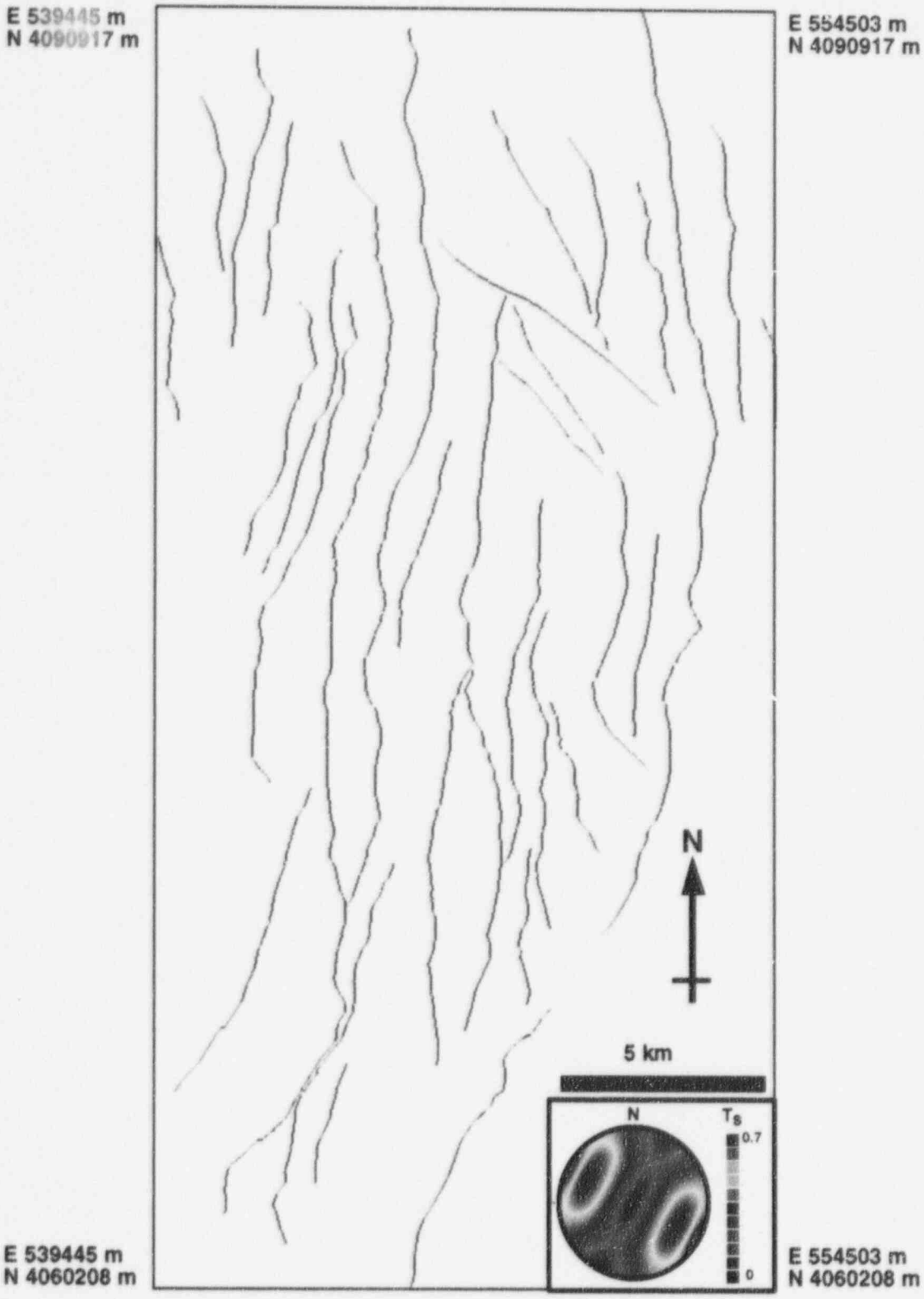

Figure 3–5. (b) Slip tendency analysis of Type I Faults shown in Figure 1–2

Although most faults in the YMR have high slip tendency in the contemporary stress state, east-west trending faults in the Ammonia Tanks resurgent dome (Sawyer et al., 1994) north of YMR have low slip tendency with respect to both modeled stress states [Figures 3-3(a) and 3-3(b)]. These faults formed in the resurgent dome, between 11.45 and 9.4 m.y. ago (Sawyer et al., 1994) in a locally nearly uniaxial stress state dominated by vertical σ_1, when the dome was uplifted. In such a stress state, steeply dipping normal faults of virtually any strike could have formed and been active.

Examination of Figures 3-3(b) and 3-4 reveals that nearly all faults at YMR that have evidence of late Quaternary displacement are in orientations of high slip tendency. For example the Crater Flat (CF), Windy Wash (WW), Solitario Canyon (SC), Fatigue Wash (FW), and SCR faults (see Figures 1-1 and 1-2 for comparison) all have high slip tendency and show evidence of Quaternary displacement. Several notable exceptions in the immediate vicinity of YM are the PWF, SW, and YWF faults. These three faults lack significant evidence of late Quaternary slip and are in low slip tendency orientations in the contemporary stress field. Therefore, it is unlikely these faults will slip in the existing stress displacement state.

Many of the regional faults with evidence of Quaternary displacement are favorably oriented in the modeled stress state (Figure 3-5). Notable exceptions are portions of the Rock Valley fault system and the Furnace Creek (FC) fault. As shown in Figure 3-5(a), the latter has a high slip tendency when it is modeled with a more appropriate stress state, dominated by E-W trending σ_3 (Zoback et al., 1992).

3.5 EFFECTS OF SUBSURFACE FAULT GEOMETRY AND SLIP TENDENCY ON EARTHQUAKE RUPTURE AREA

The maximum earthquake magnitude for a fault directly scales with the potential rupture area of the host fault (Wells and Coppersmith, 1994). Although lateral trace lengths of exposed faults are relatively well characterized in the YMR area, their down-dip extent and subsurface geometries remain unconstrained. The potential rupture areas of faults in the YMR, even those within and bounding the proposed repository, are unknown. Two cross sections of BM, Crater Flat, and YM illustrate alternative interpretations of the subsurface extent and geometry of YMR faults (Figure 3-6a,b). The dominant difference between the two interpretations is that, in the first section, the high angle faults mapped at the surface flatten into a detachment at a depth of about 7 km. In the second interpretation, high angle faults that cut YM at the surface span the entire brittle upper crust.

Slip tendency analyses of simplified versions of these two sections (Figure 3-7a,b) illustrate the dramatic effect fault geometry has on the area of a fault with higher slip tendency. In the interpretation with the detachment at 7 km (Figure 3-7a), a smaller fault surface area is in a higher slip tendency orientation than in the second interpretation, in which faults span the entire brittle crust. Finite-element analyses by Ofoegbu and Ferrill (1995) indicated that seismic slip on faults above a relatively shallow (e.g., 7 km) detachment may be limited to the high angle portions of faults. The detachment limits the areal extent of high slip tendency fault segments and, therefore, limits earthquake magnitude by reducing the size of the potential rupture area. In contrast, a system of steeply dipping faults that span the entire brittle crust (Figure 3-7b) have large surface areas with high slip tendency and, thus, a greater potential for generating large-magnitude earthquakes.

Slip tendency analysis of faults in the YMR demonstrates the critical importance of fault orientation and three-dimensional fault geometry for potential earthquake risk at the proposed repository

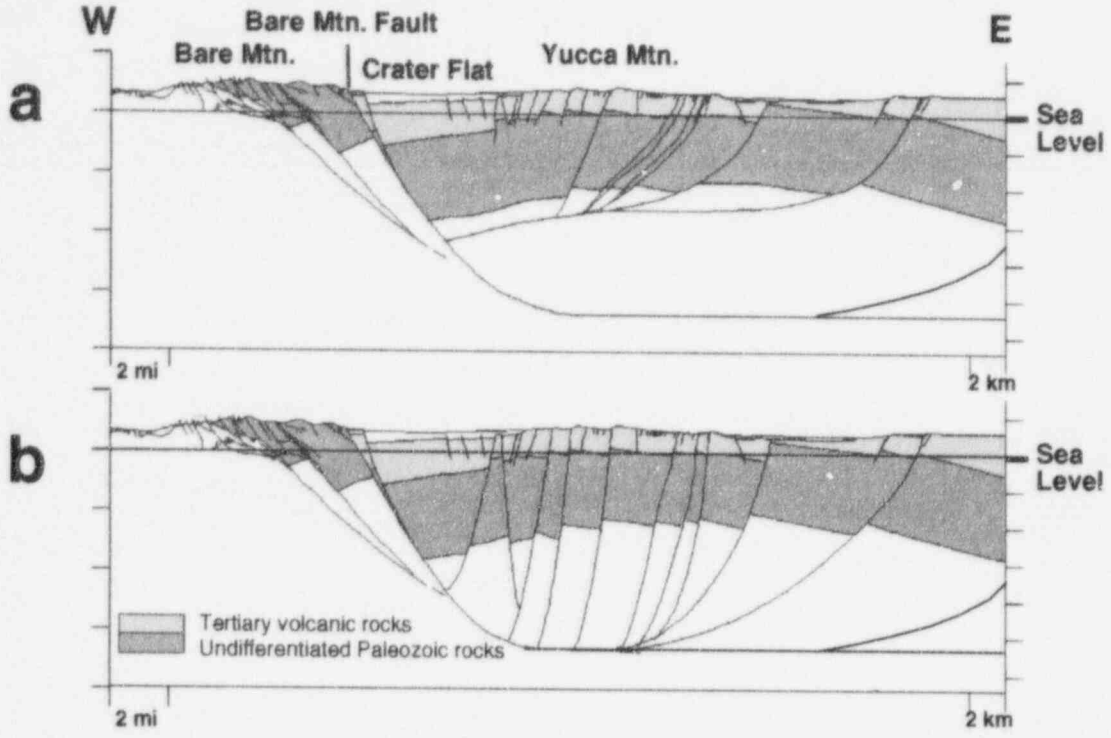

Figure 3–6. Two cross sections of Bare Mountain, Crater Flat, and Yucca Mountain illustrating alternative interpretations of the possible interaction of Yucca Mountain faults and Bare Mountain fault at depth beneath Crater Flat (Ferrill et al., 1996b). See Figure 3–2(a) for location of sections.

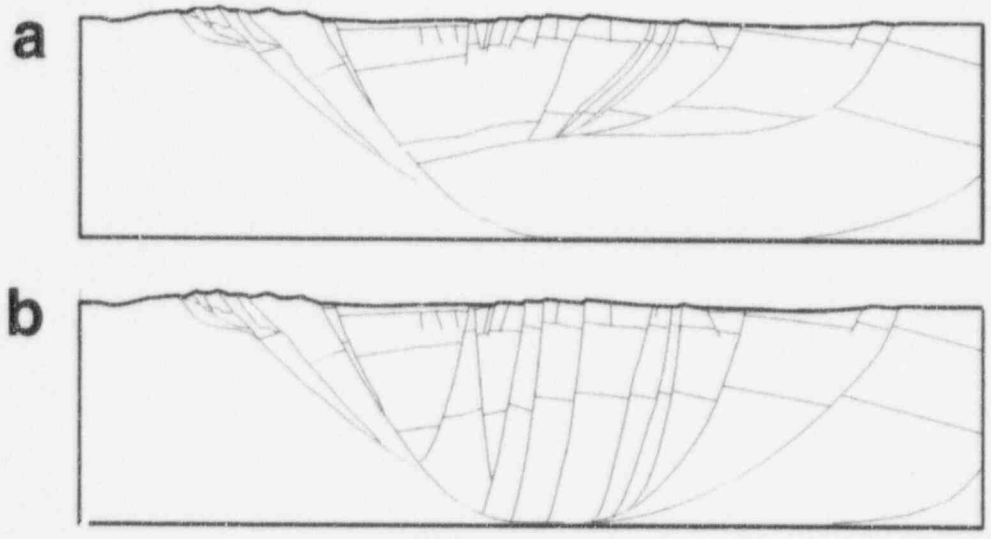

Figure 3–7. Slip tendency analysis of two cross sections illustrated in Figure 3–6. Color scale is same as in Figures 3–1 and 3–2b. The relatively small depth extent of potential high slip tendency rupture area in (a) compared with (b) suggests that configuration (a) may pose less potential seismic hazard for the proposed repository site than would configuration (b).

site. The PWF, SW, and YWF faults are poorly oriented for slip in the contemporary stress field. These faults may not have been active since the Miocene, prior to about 10 Ma, at which time the least principal stress was SW-NE, as described by Zoback et al. (1981). Interpretations of YM fault geometries in which YM faults are planar and span the entire thickness of the brittle crust may overestimate seismic risk. However, slip tendency analysis indicates that most small and large faults at YMR are favorably oriented for slip in the contemporary stress field.

4 CAVEATS AND LIMITATIONS OF FAULT CLASSIFICATION

In the selection of Type I faults from the catalog of regional and local faults, two underlying assumptions are that (i) all faults that may have a potentially significant impact on repository performance have been identified by current geological mapping, and (ii) fault lengths (which are used to determine the maximum magnitude earthquake) are reasonably represented by these maps. Most faults in the region are at least partially buried by Quaternary alluvium. As a result, their actual extent may be imprecisely known from surface mapping. Alluvium may also completely obscure significant faults within the region. Fault lengths are generally proportional to displacement and, thus, length-displacement scaling relationships can be used to highlight those faults in the data set that are anomalous because their mapped trace-lengths are either too long or too short for accumulated displacement, or displacement estimates are incorrect for the fault length. It is also important to note that the Type I fault classification does not address the role faults play in groundwater flow, thermal perturbations, or refluxation. The classification is also limited to the current location of the repository footprint. The classification here also does not include other potential seismic sources, namely those blind or hidden faults predicted by some of the viable tectonic models for the YMR.

4.1 FRACTAL SCALING RELATIONSHIPS

Numerous observations of displacements (D) and fault trace lengths (L) in well-delineated faulted terranes (Scholz and Cowie, 1990; Marrett and Allmendinger, 1991; Walsh et al., 1992; Dawers et al., 1993) show a scale-invariant power law of the form

$$D = PL^c \tag{4-1}$$

where c is the fractal dimension and P is a proportionality constant related to rock properties. Less certain is the exact value of the fractal dimension and whether or not a single power law relationship exists throughout the entire range of fault lengths and displacement magnitudes (Nicol et al., 1995). Fossen and Rørnes (1995) show distinct slopes for different scale segments of log-log plots of cumulative frequency versus fault throw for faults in the North Sea. However, Yielding et al. (1995) demonstrate scale invariance from synthetic models of faulting. The limitation of natural data according to Yielding et al. (1995) appears to be the sensitivity of fault length measurements to practical resolution of fault tips. Values of c are commonly cited as $c = 1.0$ (Dawers et al., 1993) or $c = 1.5$ (Marrett and Allmendinger, 1992). A recent review of eleven data sets of faults worldwide using more rigorous regression analysis supports a value of $c = 1.0$ (Clark and Cox, 1995).

The assumption that faults in the YMR should follow a power law scaling relationship with $c = 1.0$ provides an independent means to evaluate the fault-trace lengths used to differentiate Type I faults. In this analysis, we define a reasonable range of displacement/fault-trace length ratios based on a linear power law ($c = 1.0$) with P values between 0.01 and 0.10 (Figure 4-1). This range in P is consistent with numerous empirical results for brittle rocks (Cowie and Scholz, 1993; Dawers et al., 1993; Dawers and Anders, 1995; Yielding et al., 1995). Faulting in more ductile rocks, like salt, or very large faults ($L \geq 100$ km) tends to yield larger P values, up to $P = 0.50$ (Cowie and Schultz, 1993).

Overlain on a log-log graph of fault throw versus fault trace length (Figure 4-1) are fault data from Piety (1996) and Simonds et al. (1995) for faults that have dominant dip-slip displacements and

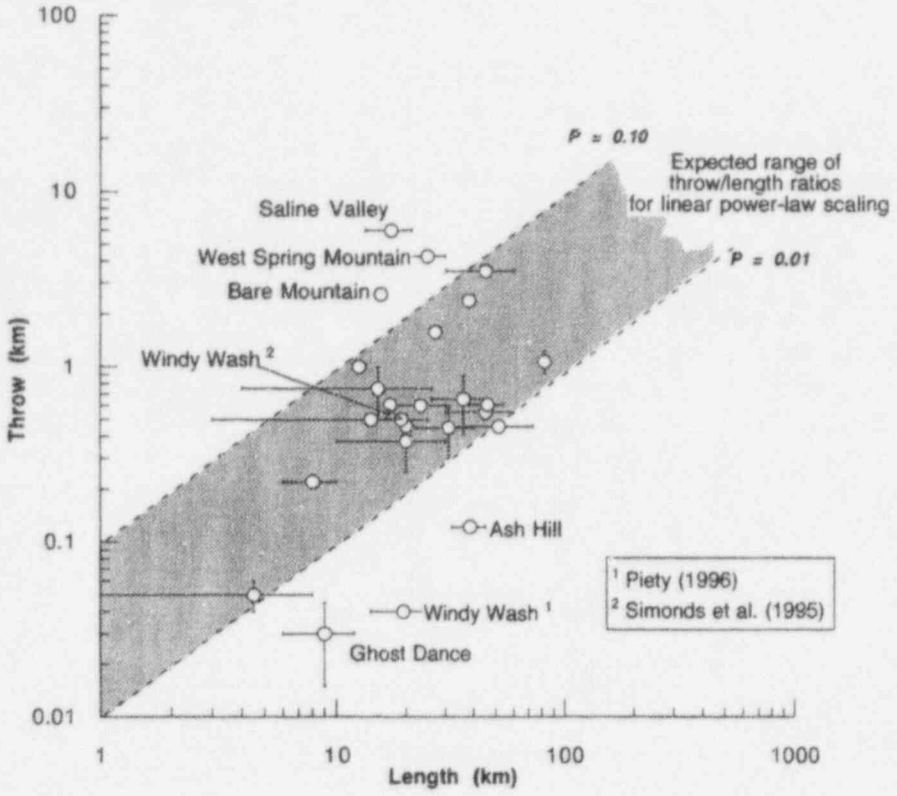

Figure 4-1. Log-log plot of fault throw as a function of fault trace length assuming a scale invariant power-law scaling relationship. Shaded region shows expected range of fault throw and fault length assuming values of $0.10 \leq P \leq 0.01$. Data are from Table 4-1.

geologically defined maximum offsets (Table 4-1). For faults where there are significant differences between fault length and displacement for both Piety (1996) and Simonds et al. (1995), both sets of values are listed (Table 4-1) and plotted (Figure 4-1). In this analysis, displacement simply refers to the vertical component (throw). Because normal faults are rarely vertical but dip between 60° and 90°, actual displacements (parallel to the fault surface) can be up to 15 percent greater than reported. For consistency, throw is used as a measure of displacement. The error bars in Figure 4-1 denote ranges in displacement or fault-trace length as reported in Piety (1996) or Simonds et al. (1995). Of 24 faults evaluated (including both Type I and Type III faults), 18 fall within the expected range. The remaining faults appear to be too short [BM, West Spring Mountain (WSM), and Saline Valley (SV)] or too long [Ghost Dance (GD), WW, and Ash Hill (AH)] for the amount of accumulated throw.

All three faults that appear too short for the amount of accumulated offset are range-front faults in which the actual fault tips are not precisely known or the faults merge into other faults with complex motions. The SV fault merges with and transfers motion to the Hunter Mountain fault (right lateral strike-slip motion) at the southern end of the Saline Valley (Burchfiel et al., 1987). The BM and WSM are both major range-front faults that appear to terminate in Quaternary (including Holocene) alluvium. Profiles of Basin and Range range-boundary dip-slip faults typically show maximum displacement near the center of the faults (Cowie and Scholz, 1993; Dawers and Anders, 1995). At BM, maximum Quaternary displacement appears to be near its mapped terminus in southern Crater Flat (Ferrill et al., 1996a;

Table 4-1. Fault lengths and throws for dip-slip faults of the Yucca Mountain region

Fault	Length (km)	Length Range (km)	Throw (km)	Throw Range (km)
Airport Lake (P)	45.00	±15.00	0.550	±0.0500
Ash Hill (P)	38.50	± 6.50	0.122	—
Bare Mountain (P)	15.50	—	2.600	±0.200
Belted Range (P)	46.00	±8.00	0.610	—
Bow Ridge (P)	8.00	± 2.00	0.220	±0.0050
Carpetbag (P)	23.25	± 6.75	0.600	—
Deep Springs (P)	27.00	—	1.575	±0.050
Emigrant Peak (P)	36.00	±10.00	0.654	±0.245
Ghost Dance (P)	9.00	± 3.00	0.030	±0.015
Grapevine (P)	25.00	± 5.00	4.270	—
Hot Creek Reveille (P)	51.50	±21.50	0.458	—
Kawich Range (P)	82.00	± 2.00	1.068	±0.153
Midway Valley (S)	4.50	± 3.50	0.050	±0.010
Oak Springs (P)	20.00	± 1.00	0.458	—
Paintbrush (P)	20.00	±10.00	0.375	±0.120
Saline Valley (P)	17.25	± 4.00	6.000	—
Solitario Canyon (P)	12.50	± 0.50	1.000	—
Solitario Canyon (S)	19.00	—	0.500	—
Stagecoach Road (S,P)	15.00	11.00	0.75	± .25
Towne Pass (P)	38.00	—	2.380	—
West Spring Mt. (P)	45.00	±15.00	3.500	—
Windy Wash (P)	19.50	± 5.50	0.040	—
Windy Wash (S)	14.00	11.00	0.500	—
Yucca (P)	31.00	± 9.00	0.450	±0.150
Yucca Lake (P)	17.00	—	0.610	—

(P) Data from Piety (1996) and (S) Data from Simonds et al. (1995).

Connor et al., 1996). Thus, the actual southern tip of the BM probably occurs well south (perhaps as much as 15 km or more) of the southern margin of Crater Flat under the alluvium of the Amargosa Desert. Doubling the current mapped length of the BM from 15.5 to 31.0 km would bring its displacement-length ratio within the expected range (Figure 4-1). Using this greater length increases M_w from 6.6 to 6.8 (an approximately 50 percent increase in energy release) and increases the peak acceleration at YMR from 0.31 to 0.34 g.

There are two possibilities to explain the three faults that appear too long for the amount of displacement. The first possibility is that these faults are actually composed of a series of fault segments that were linked together by incorrectly projecting them across covered contacts during mapping or by physical linkage as the faults grew together with time. The latter is probably the case for the AH fault, which can easily be interpreted as two distinct faults segments (each about 15 km long) with up to a 3 km gap between segments (Piety, 1996). This may also be the case for the GD and WW faults. The GD fault appears to be composed of distinct fault segments separated by zones of diffuse deformation (Scott and Bonk, 1984). The WW fault is mapped on the basis of numerous discrete alluvial scarps and is otherwise covered along most of its mapped length (Frizzell and Shulters, 1990; Scott, 1990). If this possibility is correct, then maximum magnitude and acceleration at the proposed repository site are overestimated by using the current measurements of fault-trace length. In this study, the segments of the FW fault were linked together to give an overall length of 33 km and an associated M_w of 7.7. Pezzopane (1995) provides the length as 17 km and an associate earthquake with a M_w of 6.5.

The second possibility is that the reported accumulated displacement is incorrect. The 30 m of displacement of the GD fault is the maximum observed in outcrop at the surface. Preliminary interpretations of the seismic survey across YMR (Brocher, 1994) suggests the possibility of greater than 500 m of offset across the GD fault at depth. This difference could represent possible deposition of the tuff units during faulting (growth) so only the most recent faulting is captured by measured offsets at the surface. Similarly, the displacement of the WW fault is based on offset Pliocene basalt and thus does not include possible greater offset of older units. If this possibility is correct, then current estimates of the seismic parameters (Appendix A) of these faults may be realistic.

4.2 CONCEPTUAL TECTONIC MODELS

Assumptions inherent in classifying faults as either Type I, Type II, or Type III are ultimately constrained by interpretations made from a conceptualization of the regional tectonic setting. The scaling relationships used in defining the maximum moment magnitude from the length of a mapped fault trace, for example, depend on a given depth and orientation of the fault plane. In formula presented in Section 2.4, faults were assumed to be planar with relatively steep dips that extend to the base of seismogenic crust ($\sim$15 km) because this geometry represents a reasonably simple and conservative approach. However, not all viable tectonic models for the YMR envision such deep faults. In some interpretations, many faults only extend through the upper half of the seismogenic crust ($\sim$ 6 km). Because the rupture area is smaller on such faults, maximum magnitude earthquakes expected from these faults are also smaller. In this study, only those faults or portions of faults with mapped fault traces were considered. Faults proposed in viable tectonic models that are not recognized on geologic maps, buried faults, or portions of faults with buried segments were not considered. Therefore, the reliability of this or any report that identifies faults that may pose significant risk to the performance of the proposed repository at YMR must be judged within the context of viable tectonic models of the surrounding region.

Structurally, Crater Flat is interpreted as a half-graben bounded on the west by the east-dipping BM (a first-order range-bounding normal fault) and on the east by a series of antithetic west-dipping normal faults east of YMR in Jackass Flat (e.g., Fridrich, 1996; Scott, 1990). The upper enveloping surface of the basin (defined by the top of the Miocene tuff sequence) is highest at the crest of YMR and drops in elevation westward into Crater Flat. Overall, this change in elevation defines an antithetic rollover of the hangingwall into the BM. Geometrically, the variable dips of structural blocks between YMR and rollover into the BM indicates that the BM is listric at depth. Depth to the detachment horizon is loosely constrained between about 6 km and the top brittle-ductile transition at 15 km (Young et al., 1993; Ferrill et al., 1996b). Post-Miocene alluvial thickness is greatest near the BM, defining an asymmetric basin consistent with the half-graben interpretation of Crater Flat.

Numerous classes of tectonic models have been proposed to explain the geologic setting of YMR including (i) collapsed Miocene calderas or a continental rift system (Carr, 1990; Carr and Parrish, 1985), (ii) moderate to shallow detachment fault systems with breakaways east of YMR and roots somewhere to the west of BM (Hamilton, 1988; Scott, 1990), (iii) a large Mesozoic synclinorium cut by minor Cenozoic normal faults (Robinson, 1985), (iv) a pull-apart basin or modified pull-apart basin related to first-order dextral strike-slip faulting (Fridrich 1996; Schweikert, 1989; Caskey and Schweikert, 1992), and (v) an extensional half-graben in the hangingwall above a listric BM (Ferrill et al., 1996b). Of these alternatives, the latter two (iv and v) are presently considered most viable. The structure of Crater Flat described above fits both interpretations. Details of faults and faulting in these models pose important implications for the evaluation of faults in the YMR as potential seismic hazards, primarily because of the different scaling relationships that emerge from these different tectonic models.

4.2.1 Pull-Apart Models

Pull-apart basins form by localized horizontal extension in response to extensional bends, en-echelon step-overs, or terminations of strike-slip fault systems [Figure 4-2(a)]. Pull-apart basins are generally rhombohedral in plan view and bounded on their opposite sides by normal faults. The basins terminate downward along either a horizontal detachment (Burchfiel et al., 1987) or within the brittle-ductile transition in the middle crust (Serpa et al., 1988). Often the basins are asymmetric forming as half-grabens with a single master normal fault on one margin and a series of oppositely dipping subordinate normal faults on the opposing margin [Figure 4-2(a),(b)]. In addition, the basins may also be cut by cross-basin strike-slip faults with either synthetic or antithetic sense of slip [Figure 4-2(c)] (Freund, 1970; Ron et al., 1984; Stamatakos, et al., 1988). This complex interaction of strike-slip and normal faults presents an array of potential seismic sources.

Proposed pull-apart basin models for Crater Flat include a full pull-apart or diffuse zone of transtensional shear within a larger northwest trending dextral shear zone [the Amargosa Shear of Schweikert (1989) shown in Figure 4-3(a)] or a modified pull-apart or sphenochasm structurally pinned along the northern margin of Crater Flat [Fridrich, 1996 shown in Figure 4-3(b)]. Both models are based largely on circumstantial geological evidence including clockwise vertical-axis rotations from paleomagnetic (Hudson et al., 1994; Rosenbaum et al., 1991), aeromagnetic, and gravity data that show alignment with mapped right-lateral faults to the southeast, and secondary strike-slip faults within the northeast corner of the basin. While all these features are consistent with a strike-slip controlled pull-apart basin, no one has yet provided direct evidence of a through-going or terminated strike-slip fault in Crater Flat. In fact, if such a fault exists, it must be detached below the Miocene Oasis Valley-Timber Mountain caldera complex north of Crater Flat because the plan view pattern of the caldera complex appears to be

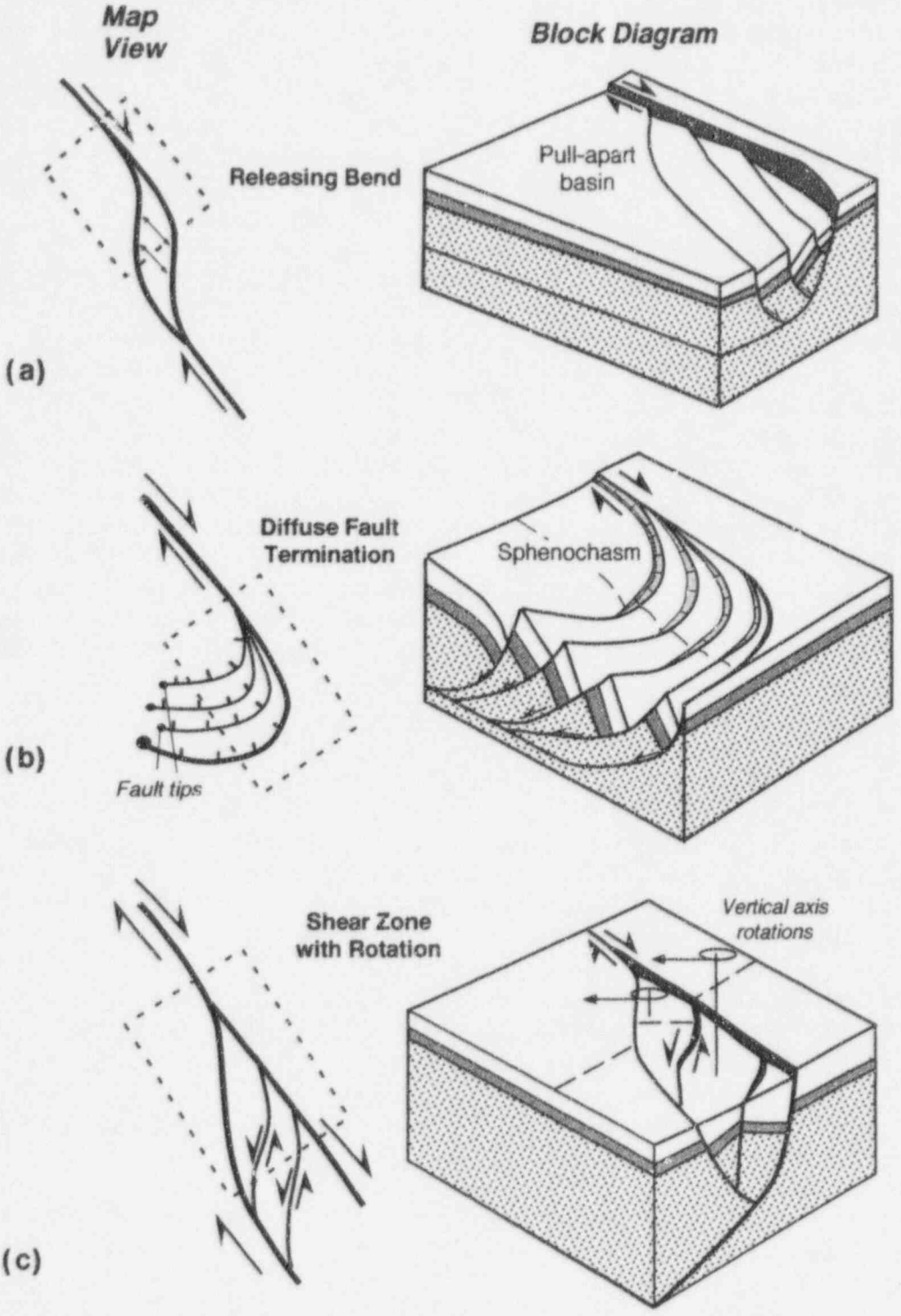

Figure 4-2. Map view and corresponding block models of strike-slip deformation. (a) A pull-apart basin formed along a releasing bend in a right-lateral strike-slip fault. (b) A sphenochasm formed at the termination of a right-lateral strike-slip fault. (c) Vertical axis block rotations with cross-basin strike-slip faults formed with a zone of right-lateral shear.

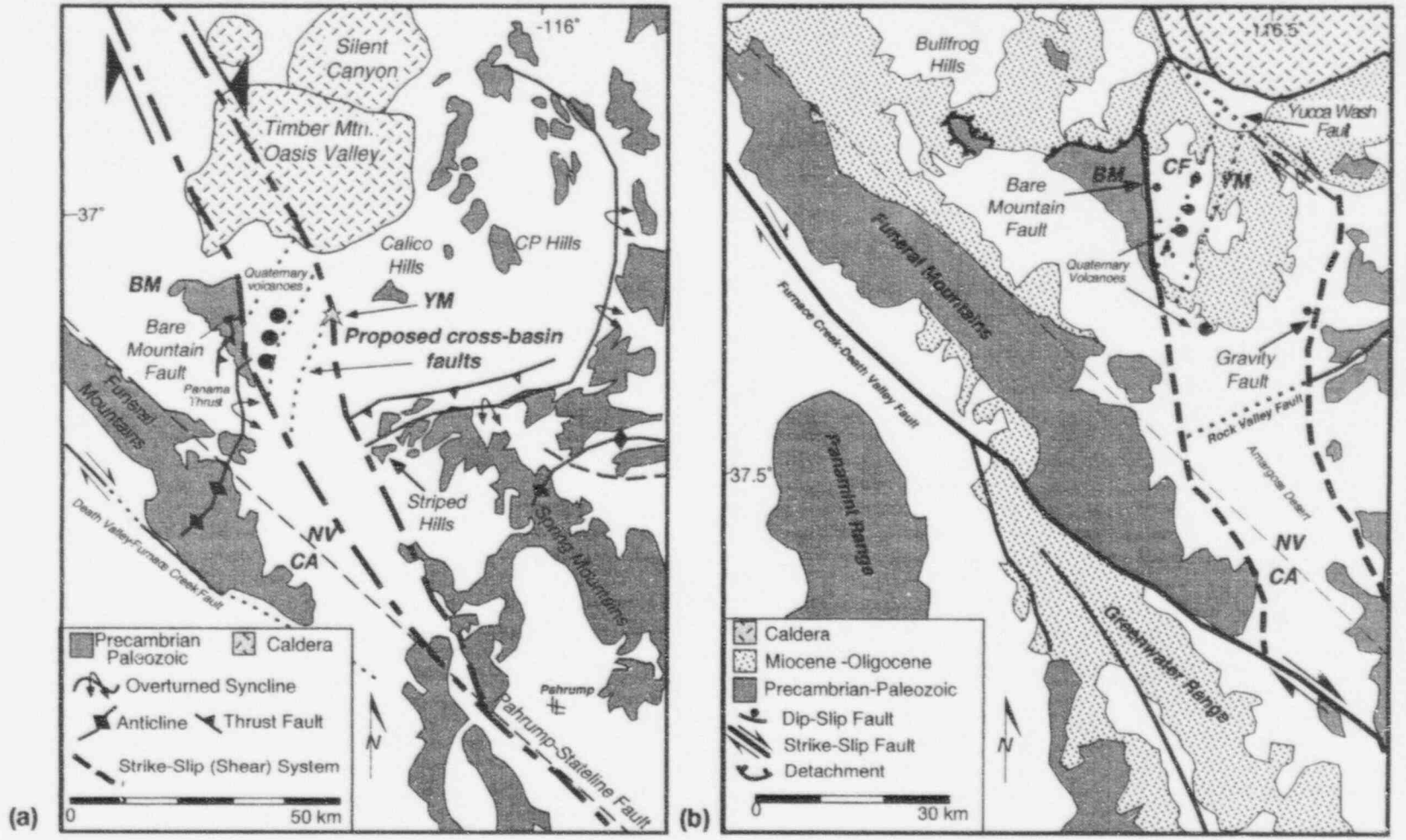

Figure 4-3. Geologic maps of Yucca Mountain (YM) from Caskey and Schweikert (1992) and Fridrich (1996) showing their interpretations of regional tectonics. (a) Amargosa shear model of Schweikert (1989). The shear is an extension of the Pahrump-Stateline fault and is based in part on restoring the fold and Panama Thrust at Bare Mountain (BM) with similar structures at the Striped Hills. Cross-basin faults, which according to Schweikert's model controlled the location of Quaternary basaltic magmatism, are also shown. (b) Sphenochasm of Fridrich (1996) showing the termination of the pull-apart basin in North Crater Flat (CF).

intact. A concealed strike-slip fault south of Crater Flat is more tenable because the region is extensively covered by Quaternary (including Holocene) alluvium.

The possibility of a major through-going or terminated strike-slip fault presents an additional seismic source not currently accounted for in the list of Type I faults. Although these faults, if they exist, have low probability for rupture they pose significant potential consequences on the seismic hazard of the proposed repository. These potential faults have not been included in the list of Type I faults because they do not meet the minimum criteria (i.e., evidence for Quaternary slip). Yet, because of their potential consequences, they need to be considered in future Probalistic Seismic Hazard Analysis (PSHA) evaluations. In the Amargosa Shear model, the proposed fault may extend more than 200 km from well southeast of Pahrump, Nevada to northwest of the Miocene caldera complex and have accumulated more than 30 km of offset. Such a fault would be of similar length and orientation to the Death Valley-Furnace Creek fault and would be capable of generating similarly large magnitude ($M_w \geq 7.8$) earthquakes with a potential hypocenter within a few kilometers of YM. If such a buried strike-slip fault were centered within Crater Flat as proposed by Schweikert (1989), its nearest approach to the proposed repository would be less than 8 km, resulting in an estimated 0.74 g or larger acceleration.

A second set of unmapped but inferred faults predicted by the pull-apart models of Schweikert (1989) and Fridrich (1996) is the secondary synthetic and antithetic strike-slip faults that cut across the basin and accommodate vertical axis (block) rotation (Freund, 1970; Ron et al., 1984; Stamatakos et al., 1988). These faults [Figure 4-3(a)] have also been called upon to explain the alignment of Quaternary volcanic centers in Crater Flat (Schweikert, 1989; Fridrich, 1996). If these faults extend across the basin, then they have lengths of about 20 km and are capable of generating earthquakes $M_w = 6.6$. An earthquake on one of these faults 2 km from YMR would result in an acceleration at the proposed repository site of 0.76 g.

Recent apatite fission track data (Ferrill et al., 1996b) do not support a reconstruction of the Striped Hills with BM and thus questions the existence of the Amargosa Shear. The pull-apart model of Fridrich (1996) is more tenable with existing data (Stamatakos and Ferrill, 1996), although more evidence of basin-bounding and cross-basin faults is needed to validate this interpretation. Future refinement of the conceptual tectonic models, as well as better characterization of potentially significant blind seismic sources and more robust treatment of seismic attenuation, is required before their influence on seismic design issues and total system performance can be evaluated.

4.2.2 Extensional Half-Graben Models

Alternatives to tectonic models that invoke strike-slip deformation are those that envision Crater Flat as an extensional basin. In this interpretation, the BM is the dominant extensional dip-slip fault. It has moderate to steep dips near the surface but becomes listric at depth, probably near the bottom of the brittle crust ($\sim$15 km) (Young et al., 1993). YM faults are subordinate to the BM and accommodate extension in its hangingwall (Figure 3-6). In these models, the noted vertical axis rotations (Hudson et al., 1994; Rosenbaum et al., 1991) reflect differential amounts of slip southward along fault planes that flatten laterally from north to south in YM and Crater Flat (Scott, 1990). The rotations occur along steeply inclined axes normal to the fault planes.

In these alternative models, the vertical extent of the faults (depth within the brittle crust) can vary depending on assumptions about the nature of the fault linkage within the hangingwall and the type

of deformation mechanism by which these faults accommodate hangingwall strain (Figure 3-6). The greatest seismic risk is for models that call on YM faults to intersect the listric segment of the BM fault [Figure 3-6(b)]. However, if the rollover of the hangingwall in Crater Flat is accomplished by outer arc extension (akin to bending of a rigid beam) then YM faults may only cut the upper part of the brittle crust and displacement on those faults would diminish with depth. In this case, the seismic risk of many faults near YM would be reduced because the small rupture areas and low slip rate of faults would be incapable of generating significantly large magnitude earthquakes (see Section 3.5).

5 SUMMARY

The following ten observations can be drawn from our quantitative and qualitative assessment of Type I Faults in the YMR:

- Of the 56 faults previously categorized as Type II faults (McKague, 1996), 52 are Type I based on the criteria established in NUREG-1451 (McConnell et al., 1992). Discriminating characteristics of Type I faults are: (i) fault displacement(s) in the Quaternary, (ii) favorable orientation of the fault planes for future slip relative to the modern stress field, and (iii) estimated peak acceleration equal to or greater than 0.1 g at the proposed YMR repository site.

- Faults which have previously been deemed as Type II (McKague, 1996) and were not considered Type I in this report are the PWF, SW, and YWF faults. These three northwest-trending faults were classified as Type III based on a lack of significant evidence for Quaternary slip and their relatively low slip tendency values within the current stress field.

- The BS fault was classified as the only remaining Type II fault because of differing opinions on its origin.

- Of the 52 Type I faults, the 24 which produce the greatest estimates of peak acceleration at the proposed repository site lie within a 10 km radius of YMR. This is not surprising considering the sensitivity of peak acceleration values to proximity of the fault to the proposed repository site. Other faults that also show significant accelerations include the BM, SCR, and RV faults (all with g values greater than 0.25).

- Comparisons of fault-trace lengths to cumulative vertical displacement (throw) for dip-slip faults in the YMR are consistent with linear power-law scaling relationships established from fault data sets worldwide. Important exceptions in this analysis are the BM, GD, and WW faults.

- The 15.5 km mapped fault-trace length for the BM appears too short for its greater than 2.5 km of throw, suggesting that the fault may extend well south of Crater Flat under the Amargosa Desert alluvium. Re-evaluation of the seismic potential for a 31.0-km-long BM suggest an increase of the maximum magnitude earthquake from M_w=6.6 to M_w=6.8 and a slight increase in the peak acceleration at the YMR site from 0.31 to 0.34 g.

- The GD and WW faults appear to be too long for current estimates of throw, suggesting that either these estimates significantly under-represent actual offset or that the two faults are actually composed of a series of distinct smaller fault segments. If the latter is correct, then seismic hazard assessments may overestimate the earthquake moment magnitudes from these two faults.

- In addition to mapped faults, consideration of viable tectonic models for the YMR suggests the presence of several significant blind seismic sources. For example, the Amargosa Shear model of Schweikert (1989) suggests a buried strike-slip fault beneath Crater Flat that has the potential for a M_w=7.8 earthquake and a peak acceleration at the proposed repository of 0.76 g. Similarly, the pull-apart models of Fridrich (1996) include the possibility of 20–30-km-long

strike-slip faults (including an active YWF fault) with the potential of M_w=6.6 to M_w=6.8 magnitude earthquakes and peak accelerations of between 0.65 and 0.74 g. Recent apatite fission-track ages from Bare Mountain (Ferrill et al., 1996b) do not support a reconstruction of the Striped Hills and Bare Mountain and thus raise doubt about the existence of the Amargosa Shear. In contrast, the pull-apart model of Fridrich (1996) appears more tenable. However, more direct evidence of basin-bounding and cross-basin strike-slip faults is needed to validate their existence.

- In alternative conceptual tectonic models (Ferrill et al., 1996b), faults within and adjacent to YMR may not extend to the base of the seismogenic crust but either sole into a moderate detachment or tip-out down dip (i.e., the amount of displacement may be maximum at the surface but systematically lessen downward to a point of zero offset at a middle-upper crustal level). Rupture areas of these faults may therefore be smaller than present estimates, thus reducing the potential for large earthquakes. If correct, then the seismic risk of these faults may be overestimated.

- Assessment of the role of faults in repository design and performance is a complex interaction of data, its interpretation, and modeling. This study provides the basis and preliminary data for use in bounding analyses of structural deformation. Future refinement of the conceptual geological models as well as better characterization of these potentially significant blind seismic sources is required to fully appraise their influence on repository safety and performance.

6 REFERENCES

Abrahamson, N.A., and J.J. Litehiser. 1989. Attenuation of vertical peak acceleration. *Bulletin of the Seismological Society of America* 79: 549–567.

Anderson, L.W., and R.E. Klinger. 1996. The Beatty Scarp in Nye County, Nevada—An important Late Quaternary morphologic datum. *Bulletin of the Seismological Society of America* 86: 1,650–1,654.

Bellier, O., and M.L. Zoback. 1995. Recent state of stress change in the Walker Lane zone, western Basin and Range Province, United States. *Tectonics* 14: 564–593.

Boore, D.M., W.B. Joyner, and T.E. Fumal. 1993. *Estimation of response spectra and peak accelerations from western North American earthquakes; An interim report*. U.S. Geological Survey Open File Report 93-509. Denver, CO.

Boore, D.M., W.B. Joyner, and T.E. Fumal. 1994. *Estimation of response spectra and peak accelerations from western North American earthquakes; An interim report part 2*. U.S. Geological Survey Open File Report 94-127. Denver, CO.

Brocher, T. 1994. *Seismic Reflection Investigations. Major Results of Geophysical Investigations at Yucca Mountain and Vicinity, Southern Nevada*. H.W. Oliver, D.A. Ponce, and W. Clay-Hunter eds. U.S. Geological Survey Open File Report 96-28. Menlo Park, CA.

Burchfiel, B.C., K.V. Hodges, and L.H. Royden. 1987. Geology of Panamint Valley-Saline Valley pull-apart system, California: Palinspastic evidence for low-angle geometry of a Neogene range-bounding fault. *Journal of Geophysical Research 92*: 10,422–10,426.

Byers, F.M. Jr., W.J. Carr, P.P. Orkild, W.D. Quinlivan, and K.A. Sargent. 1976. *Volcanic suites and related cauldrons of Timber Mountain - Oasis Valley Complex, Southern Nevada. U.S.* Geological Survey Professional Paper 919. Washington, DC.

Campbell, K.W. 1981. Near-source attenuation of peak horizontal acceleration. *Bulletin of the Seismological Society of America* 71: 2,039–2,070.

Campbell, K.W. 1987. Predicting strong ground motion in Utah. *Evaluation of Regional and Urban Earthquakes and Risk in Utah*. W.W. Hays and P.L. Gori, eds. U.S. Geological Survey Professional Paper 87-585II, L1-L90. Washington, D.C.

Campbell, K.W. 1989. Empirical prediction of near-source ground motion for the Diablo Canyon power plant site, San Luis Obispo County, California. U.S. Geological Survey Open-File Report 89-484. Denver, CO.

Campbell, K.W. 1993. Empirical prediction of near-source ground motion from large earthquakes. *Proceedings of the International Workshop on Earthquake Hazard and Large Dams in the Himalaya*. V.K. Gaur, ed., Indian National Trust for Art and Cultural Heritage, New Delhi. 93–103.

Carr, W.J. 1990. Styles of extension in the Nevada Test Site region, southern Walker Lane Belt; An integration of volcano-tectonic and detachment fault model. *Geological Society of America Memoir* 176: 283–303.

Carr, W.J., and L.D. Parrish. 1985. *Geology of Drill Hole USW-VH-2 and Structure of Crater Flat, Southwestern, Nevada*. U.S.Geogical Survey Open File Report 85-475. Denver, CO:

Caskey, S.J., and R. Schweikert. 1992. Mesozoic deformation in the Nevada Test Site and vicinity: Implications for the structural framework of the Cordilleran fold and thrust belt and Tertiary extension north of Las Vegas Valley. *Tectonics* 11: 1,214–1,331.

Clark, R.M., and S.J.D. Cox. 1995. A modern regression approach to determining fault displacement-length scaling relationships. *Journal of Structural Geology* 18: 147–152.

Code of Federal Regulations. 1996. Disposal of High-Level Radioactive Waste in Geologic Repositories. Part 60, Chapter I, Title 10, Energy. Washington, D.C.

Connor, C.B., R.H. Martin, P.G. Hunka, J.A. Stamatakos, D.B. Henderson, and R.V. Klar. 1996. *Ground Magnetic Survey of the Little Cones, Crater Flat, Nevada*. CNWRA 96-002. San Antonio, TX: Center for Nuclear Waste Regulatory Analyses.

Cornwall H.R., and F.J. Kleinhampl. 1961. *Geology of the Bare Mountain Quadrangle*. U.S. Geological Survey Geological Quadrangle Map GQ-157, Scale 1:62,500.

Cowie, P.A., and C.H. Scholz. 1993. Displacement-length scaling relationships for faults: Data synthesis and discussion. *Journal of Structural Geology* 14: 1,149–1,156.

Dawers, N.H., and M.H. Anders. 1995. Displacement-length scaling and fault linkage. *Journal of Structural Geology* 17: 607–614.

Dawers, N.H., M.H. Anders, and C.H. Scholz. 1993. Growth of normal faults: displacement-length scaling. *Geology* 21: 1,107–1,110.

Dickerson, R. 1996. Geologic and geophysical evidence for normal faulting in Yucca Wash, Yucca Mountain, Nevada. *Geological Society of America Abstracts with Program 1996 Annual Meeting*. Boulder, Co: Geological Society of America 28(7):191.

Ferrill, D.A., S.R. Young, A.P. Morris, D.B. Henderson, and R.H. Martin. 1994. 3-dimensional stress domains interpreted from fault slip patterns in southern California and Nevada. *Geological Society of America Abstracts with Program 1994 Annual Meeting*. Boulder, CO: Geological Society of America: 26(7): 185.

Ferrill, D.A., G.L. Stirewalt, D.B. Henderson, J.A. Stamatakos, A.P. Morris, B.P. Wernicke, and K.H. Spivey. 1995. *Faulting in the Yucca Mountain Region: Critical Review and Analyses of Tectonic Data from the Central Basin and Range*. CNWRA 95-017. San Antonio, TX: Center for Nuclear Waste Regulatory Analyses.

Ferrill, D.A., J.A. Stamatakos, S.M. Jones, B. Rahe, H.L. McKague, R.H. Martin, and A.P. Morris. 1996a. Quaternary slip history of the Bare Mountain fault (Nevada) from the morphology and distribution of alluvial fan deposits. *Geology* 24: 559–562.

Ferrill, D.A., G.L. Stirewalt, D.B. Henderson, J.A. Stamatakos, A.P. Morris, B.P. Wernicke, and K.H. Spivey. 1996b. *Faulting in the Yucca Mountain Region: Critical Review and Analyses of Tectonic Data from the Central Basin and Range*. NUREG/CR-6401. Washington, DC: Nuclear Regulatory Commission.

Fossen H., and A. Rørnes. 1995. Properties of fault populations in the Gullfakes Field, northern North Sea. *Journal of Structural Geology* 18: 179–190.

Fridrich, C.J. 1996. Tectonic Evolution of the Crater Flat Basin, Yucca Mountain region, Nevada. *Geological Society of America Bulletin*. In Press.

Frizzell, V.A. Jr., and J. Shulters. 1990. *Geologic Map of the Nevada Test Site, Southern Nevada*. U.S. Geological Survey Miscellaneous Investigations Series, Map I-2046, Scale 1:100,000. Denver, CO.

Freund, R. 1970. Rotation of strike-slip faults in Sistan, southeastern Iran. *Journal of Geology* 78: 188–200.

Groshong, R.H., Jr. 1988. Low-temperature deformation mechanisms and their interpretation. *Geological Society of America Bulletin* 100: 1,329–1,360.

Hamilton, W.B. 1988. Detachment faulting in the Death Valley region, California and Nevada. Geologic and Hydrologic Investigations of a Potential Nuclear Waste Disposal Site at Yucca Mountain, Southern Nevada. M.D. Carr and J.C. Yount, eds. *U.S. Geological Survey Bulletin 1790*: 51–85.

Harding, S.T. 1988. Preliminary results of high-resolution seismic-reflection surveys conducted across the Beatty and Crater Flat Scarps, Nevada. Geologic and Hydrologic Investigations of a Potential Nuclear Waste Site at Yucca Mountain, Southern Nevada. M.D. Carr, and J.C. Yount, eds. *U.S. Geological Survey Bulletin* 1790: 121–127.

Harmsen, S.C. 1994. The Little Skull Mountain, Nevada, earthquake of 29 June 1992: Aftershock focal mechanisms and tectonic stress field implications. *Bulletin of the Seismological Society of America* 84: 1,484–1,505.

Hudson, M.R., D.A. Sawyer, and R.G. Warren. 1994. Paleomagnetism and rotation constraints for the middle Miocene southwestern Nevada volcanic field. *Tectonics* 13: 258–277.

Idriss, I.M. 1991. Earthquake ground motions at soft soil sites. *2nd International Conference on Recent Advances in Geotechnical Earthquake Engineering and Soil Dynamics* 3: 2,265–2,272.

Jaeger, J.C., and N.G.W. Cook. 1979. *Fundamentals of Rock Mechanics*. (Third Edition). Chapman and Hall, London: U.K.

Joyner, W.B., and D.M. Boore. 1981. Peak horizontal acceleration and velocity from strong motion records including records from the 1979 Imperial Valley, California, earthquake. *Bulletin of the Seismological Society of America* 71: 2,011–2,038.

Joyner, W.B., and D.M. Boore. 1988. Measurement, characterization, and prediction of strong ground motion. *Proceedings of Earthquake Engineering and Soil Dynamics: Recent Advances in Ground Motion Evaluation*. J.L. Von Thun, ed. American Society of Civil Engineers: 1–60.

Marrett, R., and R.W. Allmendinger. 1991. Estimates of strain due to brittle faulting: Sampling of fault populations. *Journal of Structural Geology* 13: 735–738.

Marrett, R., and R.W. Allmendinger. 1992. Amount of extension on "small" faults: An example from the Viking Graben. *Geology* 20: 47–50.

Martin, R. 1995. *GIS Library and Geospatial Database Description and Instructions for CDROM Version 0.12*. San Antonio, TX: Center for Nuclear Waste Regulatory Analyses.

McConnell, K.I., M.E. Blackford, and A.K. Ibrahim. 1992. *Staff Technical Position on Investigations to Identify Fault Displacement Hazards and Seismic Hazards at a Geologic Repository*. NUREG-1451. Washington, DC: Nuclear Regulatory Commission.

McKague, H.L. 1996. *Identification of Type II Faults in the Yucca Mountain Area*. Letter Report. San Antonio, TX: Center for Nuclear Waste Regulatory Analyses.

Monsen, S.A., M.D. Carr, M.C. Reheis, and P.P. Orkild. 1992. Geologic Map of Bare Mountain, Nye County, Nevada. U.S. Geological Survey Miscellaneous Investigations Map I-2201. Scale 1:24,000. Denver, CO:

Morris, A.P., D.A. Ferrill, and D.B. Henderson. 1996. Slip tendency analysis and fault reactivation. *Geology* 24: 275–278.

Nakata, J.K., C.M. Wentworth, and M.N. Machette. 1982. *Quaternary Fault Maps of the Basin and Range and Rio Grande Rift Provinces, Western United States*. Scale 1:2,500,000. U.S. Geological Survey Open File Report 82-579. Denver, CO.

Nicol, A., J.J. Walsh, J. Watterson, and P.A. Gillespie. 1995. Fault size distributions—Are they really power law? *Journal of Structural Geology* 18: 191–197.

Ofoegbu, G.I., and D.A. Ferrill. 1995. Mechanical analyses of a Yucca Mountain fault model. *Proceedings of the Topical Meeting on Methods of Seismic Hazards Evaluation, Focus '95*. LaGrange Park, IL: American Nuclear Society: 115–124.

Fezzopane, S.K. 1995. *Preliminary Table of Characteristics of Known and Suspected Quaternary Fault in the Yucca Mountain Area*. Administrative Report. U.S. Geological Survey. Denver, CO.

Piety, L.A. 1996. *Compilation of Known and Suspected Quaternary Faults Within 100 km of Yucca Mountain*. Scale 1:250,000. U.S. Geological Survey Open File Report 94-112 (Draft). Denver, CO.

Robinson, G.D. 1985. *Structure of Pre-Cenozoic rocks in the vicinity of Yucca Mountain, Nye County, Nevada—A potential nuclear-waste disposal site*. U.S. Geological Survey Bulletin 1647: 1-22.

Ron, H., R. Freund, Z. Garfunkel, and A. Nur. 1984. Block rotation by strike-slip faulting: Structural and paleomagnetic evidence. *Journal of Geophysical Research* 89: 6,256-6,270.

Rosenbaum, J.G., M.R. Hudson, and R.B. Scott. 1991. Paleomagnetic constraints on the geometry and timing of deformation at Yucca Mountain, Nevada: *Journal of Geophysical Research* 96: 1,963-1,980.

Sabetta, F., and A. Pugliese. 1987. Attenuation of peak horizontal acceleration and velocity from Italian strong-motion records. *Bulletin of Seismological Society of America* 77: 1,491-1,513.

Sadigh, K., J. Egan, and R. Youngs. 1986. Specification of ground motion for seismic design of long period structures. *Earthquake Notes* 57: 13-14.

Sawyer, D.A., R.J. Fleck, M.A. Lanphere, R.G. Warren, D.E. Broxton, and M.R. Hudson. 1994. Episodic caldera volcanism in the Miocene southwestern Nevada volcanic field: Revised stratigraphic framework, $^{40}Ar/^{39}Ar$ geochronology, and implications for magmatism and extension, *Geological Society of America Bulletin* 106: 1,304-1,318.

Sawyer, D.A., R.R. Wahl, J.C. Cole, S.A. Minor, R.J. Laczniak, R.G. Warren, C.M. Engle, and R.G. Vega. 1995. *Preliminary Digital Geologic Map Database of the Nevada Test Site Area, Nevada*. U.S. Geological Survey. Open File Report 95-0567. Scale 1:100,000. Denver, CO.

Scholz, C.H., and P.A. Cowie. 1990. Determination of total strain from faulting using slip measurements. *Nature* 346: 837-839.

Schweikert, R.A. 1989. Evidence for a concealed strike-slip fault beneath Crater Flat, Nevada. *Geological Society of America Abstracts with Programs* 21: A90.

Scott, R.B. 1990. Tectonic setting of Yucca Mountain, southwest Nevada. Basin and range extensional tectonics near the latitude of Las Vegas, Nevada. B.P. Wernicke, ed. *Geological Society of America Memoir 176*: 251-282.

Scott, R.B., and J. Bonk. 1984. *Preliminary geologic map of Yucca Mountain, Nye County, Nevada, with geologic sections*. U.S. Geological Survey Open File Report 84-494. Scale 1:12,000. Denver, CO.

Serpa, L., B. de Voogd, L. Wright, J. Willemin, J. Oliver, E. Hauser, and B. Troxel. 1988. Structure of the central Death Valley pull-apart basin and vicinity from COCORP profiles in the southern Great Basin. *Geological Society of American Bulletin* 100: 1,437–1,450.

Simonds, W.F., J.W. Whitney, K. Fox, A. Ramelli, J.C. Yount, M.D. Carr, C.D. Menges, R. Dickerson, and R.B. Scott. 1995. *Map of Fault Activity of the Yucca Mountain Area, Nye County, Nevada*. U.S. Geological Survey Miscellaneous Investigations Series Map, 1-2520. Scale 1:24,000. Denver, CO.

Stamatakos, J., K.P. Kodama, and T.L. Pavlis. 1988. Paleomagnetism of Eocene plutonic rocks, Matanuska Valley, Alaska. *Geology* 16: 618–622.

Stamatakos, J., and D.A. Ferrill. 1996. Tectonic processes in the central basin and range region. *NRC High-Level Radioactive Research at CNWRA July–December 1995*. B. Sagar, ed. CNWRA 96-02S. San Antonio, TX: Center for Nuclear Waste Regulatory Analyses. 6-1 to 6-25.

Stock J.M., and J.H. Healy. 1987. Stress field at Yucca Mountain, Nevada. eds. M.D. Carr, and J.C. Yount. Geologic and Hydrologic Investigations of a Potential Nuclear Waste Disposal Site at Yucca Mountain, Southern Nevada. *U.S. Geological Survey Bulletin* 1,790 87–93.

Stock, J.M., J.H. Healy, S.H. Hickman, and M.D. Zoback. 1985. Hydraulic fracturing stress measurements at Yucca Mountain, Nevada, and relationship to regional stress field. *Journal of Geophysical Research* 90(B10): 8,691–8,706.

Swadley, W.C., J.C. Yount, S.T. Harding. 1988. Surficial geologic map of Bare Mountain, Nye County, Nevada. Geologic and Hydrologic Investigations of a Proposed Nuclear Waste Disposal Site at Yucca Mountain, Southern Nevada. M.D. Carr and J.C. Yount, eds. *U.S. Geological Survey Bulletin* 1790: 113–119.

Tsai, Y.B., F.W. Brady, and L.S. Cluff. 1990. An integrated approach for characterization of ground motions in PG&E's long term seismic program for Diablo Canyon. *Proceedings of the 4th U.S. National Conference on Earthquake Engineering* (1): 597–606.

Walsh J.J., J. Watterson, and G. Yielding. 1992. The importance of small-scale faulting in regional faulting. *Nature* 351: 391–393.

Wells, D.L., and K.J. Coppersmith. 1994. New empirical relationships among magnitude, rupture length, rupture width, rupture area, and surface displacement. *Bulletin of the Seismological Society of America* 84: 974–1,002.

Wernicke, B, G.J. Axen, and J.K. Snow. 1988. Basin and Range extensional tectonics at the latitude of Las Vegas, Nevada. *Geological Society of America Bulletin* 100: 1,738–1,757.

Wesnousky, S.G., and C.H. Jones. 1994. Oblique slip, slip partitioning, spatial and temporal changes in the regional stress field, and the relative strength of active faults in the Basin and Range, western United States. *Geology* 22: 1,031–1,034.

Yielding G., T. Needham, and H. Jones. 1995. Sampling of fault populations using sub-surface data: A review. *Journal of Structural Geology* 18: 135–146.

Young, S.R., G.L. Stirewalt, and A.P. Morris. 1993. *Geometric Models of Faulting at Yucca Mountain.* CNWRA 92-008. San Antonio, TX: Center for Nuclear Waste Regulatory Analyses.

Zoback, M.L., R.E. Anderson, and G.A. Thompson. 1981. Cainozoic evolution of the state of stress and style of tectonism of the Basin and Range province of the western United States. *Philosophical Transactions of the Royal Society of London* A300: 407–434.

Zoback, M.L., and 36 Project Participants. 1992. World stress map–maximum horizontal stress orientation. *Journal of Geophysical Research* 87:(B8).

APPENDIX A

SYNOPSIS OF DATA FOR 56 FAULTS IN AND AROUND THE YUCCA MOUNTAIN REGION

EXPLANATION OF APPENDIX A

Fault Name: The fault names are followed by an abbreviation used in Figures 1-1 and 1-2. Abbreviations are also listed in Appendix B. Numbered faults on figures 1-2 are from Simonds et al. (1995). Numbering was done by authors of this report to identify faults. These 18 faults are not included in Appendix B.

Source(s) of Information: Primary source listed first, secondary sources follow.

Location: Under this heading, the Figure (1-1 or 1-2) on which the fault is plotted to visualize its location relative to the repository is given.

Style of Faulting: A simple descriptor to indicate the kind of fault based on the known or assumed relative motion across the fault.

Orientation of Fault: A simple descriptor to indicate the predominant strike and dip of the fault plane. Many of the fault traces are sinuous and change strike by 30° to 45°. Dips are often poorly known, although the direction of the dip is reliable in most cases.

Maximum Fault Length: For many faults the length is well known. For others, often those that occur in alluvial valleys, the lengths may be over-or under-represented. In alluvial valleys, fault segments are often linked together assuming they are part of the same fault. This could have the effect of overestimating the lengths and underestimating the number of faults. In other cases, erosion may destroy sections of a fault resulting in a shorter estimate of the fault length. Fault lengths should be considered approximate because they depend on the scale and accuracy of the original mapping, as well as how faults and lineaments are interpreted and combined to estimate total length.

Youngest Displacement: The youngest identified displacement is given.

Maximum Displacement: This is measurable total stratigraphic displacement, but may not reflect the actual total displacement, especially when the measured displaced units are in alluvium or the younger tuffs that conceal older units which may have accumulated more displacement prior to burial by younger alluvium or tuffs.

Slip Rate: In Piety (1996) and Simonds et al. (1995) the reported slip rates appear to be determined by dividing the stratigraphic displacement by the age of the stratigraphic marker unit. The dip angle of the fault plane appears not to have been considered for dipping faults. To estimate the slip rate, the throw rate should be increased up to 15 percent for fault dips between 60° and 90°. Slip rates of strike-slip faults are correctly represented if pre-displacement correlations are correct.

Recurrence Interval: Because of the difficulty of obtaining multiple offset data, this parameter is often unknown.

Comment: Under this heading there is a statement about the potential for fault displacement in the repository. Because most faults are well beyond the repository perimeter, fault displacement is rarely a concern. Currently, only the Ghost Dance fault in the proposed repository, the Bow Ridge and Drill Hole Wash faults that intersect the north ramp of the ESF and a splay of the Solatario Canyon fault that trend into the repository need to be evaluated as to the consequences of fault displacement. In addition, there is an estimate of peak acceleration for each fault. This was calculated as a criterion for distinguishing

distinguishing Type I faults from Types II and III. The procedure used to calculate the peak acceleration is more fully described in McKague (1996). The maximum-moment (M_w) magnitude of the earthquake was calculated from the maximum length (L) of the fault using the equation from Wells and Coppersmith (1994) $[M_w = 5.08 + 1.16 \log(L)]$. The acceleration was calculated using the attenuation formula of Campbell (1987) (i.e., $\ln(A) = -2.893 + (0.85M_w) - 1.25\ln((r^2 + 16)^{1/2} + 0.0872e^{0.678M_w}) - 0.0059r$) where A is average acceleration, M_w is the maximum-moment magnitude and r is the closest approach of the fault to the refrence point at the surface. The peak acceleration is calculated by multiplying A by 1.12 and is calculated to a point on the earth's surface at 548371 m, 407744 m; Universal Transverse Mercator (UTM) coordinates. This location is refered to as the refrence point. This determination of peak acceleration is not intended to be used as any measure of the seismic hazard at the repository. To fully consider the seismic hazard at the repository, other aspects such as recurrence intervals and slip rate need to be included in the analysis. Pezzopane (1995) also included an estimate of maximum-moment magnitude calculated using the same formula from Wells and Coppersmith (1994). There appears to be close agreement between Pezzopane's values and those determined in this report. We note in Appendix A those faults which we determine M_w differs by more than 0.1 from Pezzopane's value. Differences of more than 0.1 moment magnitude units are always due to the differing estimates of fault length. Miscellaneous comments with regard to specific faults are also included under this heading.

Type I Faults

Abandoned Wash fault (AWF)

Comment: In Figure 1-2 Ghost Dance fault is linked to Abandoned Wash fault for a total length of 9 km. This fault system is characterized under the Ghost Dance fault on page A-10.

Amargosa River fault (AR)

Source of Information:	Piety, 1996
Location:	Figure 1-1
Style of Faulting:	Strike Slip Right-Lateral
Orientation of Fault:	Strike: Northwest Dip: No information
Maximum Fault Length:	About 15 km
Youngest Displacement:	Holocene
Maximum Displacement:	No information
Slip Rate:	No information
Recurrence Interval:	No information

Comment: Fault is well beyond the repository and fault displacement will not be a hazard. Peak acceleration is estimated to be 0.1 g at the surface at the refernce point. This estimate is based on a 6.4 (M_w) earthquake occurring 40 km from the refrence point.

Fault consists of a zone of discontinuous en echelon lineaments and scarps. This fault is considered a possible extension of the Pahrump fault by Donovan (1991).

Type I Faults (cont'd)

Ash Meadows fault (AM)

Source of Information:	Piety, 1996
Location:	Figure 1-1
Style of Faulting:	Dip Slip
Orientation of Fault:	Strike: North Dip: 55-58° W
Maximum Fault Length:	60 km
Youngest Displacement:	Variable along fault trace: Northern Section-Holocene; Central Section-Late Pleistocene; Southern Section-Holocene/Late Pleistocene
Maximum Displacement:	Surface: 1.55 m Bedrock: 50 m/3.2 Ma
Slip Rate:	0.016 mm/yr (vertical) (northern section) 0.04 mm/yr (vertical) (central section)
Recurrence Interval:	No information

Comment: Fault is well beyond the repository and fault displacement will not be a hazard. Peak acceleration is estimated to be 0.2 g at the surface at the refrence point. This estimate is based on a 7.1 (M_w) earthquake occurring 34 km from the refrence point.

Bare Mountain fault (BM)

Sources of Information:	Nakata et al., 1982; Piety, 1996
Location:	Figure 1-1
Style of Faulting:	Dip Slip
Orientation of Fault:	Strike: North Dip: Eastward but variable, from 45° to 55° at Tarantula Canyon to 60° to 70° south of Tarantula Canyon (Monsen et al., 1992)
Maximum Fault Length:	21.3 km (Nakata, et al., 1982), 15.5 km (Piety, 1996)
Youngest Displacement:	Holocene et al
Maximum Displacement:	Increases north to south (Ferrill et al., 1996a) Bedrock: 28/km Surface: 1.75 m
Slip Rate:	Variable. Appears to vary from 0.019 mm/yr (Klinger and Anderson 1994) at the north end to 0.20 mm/yr (Reheis, 1988) at the south end
Recurrence Interval:	20,000 to 80,000 yr

Comment: Fault is well beyond the repository and fault displacement will not be a hazard. Movement on the BM fault could cause coseismic displacement of faults within the controlled area. Peak acceleration is estimated to be 0.31 g at the surface at the refrence point. This estimate is based on a 6.6 (M_w) earthquake occurring 15 km from the refrence point. Piety (1996) suggests a maximum fault length of 15.5 km. With this length the estimated peak acceleration at the surface at the refrence point is 0.30 g. Pezzopane (1995) calculates a 6.5 (M_w) for a 16-km-long fault. Analysis of fault length to displacement relationships, in Section 4.1, indicates the BM fault is too short for the total displacement and could be at least twice as long, resulting in an increased peak acceleration of $\geq$0.34 g at the surface at the refrence point.

Type I Faults (cont'd)

Belted Range fault (BLR)

Source of Information:	Piety, 1996
Location:	Figure 1-1
Style of Faulting:	West facing scarps on east side of Kawich Valley and a large displacement, valley side down, based on a gravity interpretation, suggests a dip slip fault
Orientation of Fault:	Strike: North Dip: West
Maximum Fault Length:	54 km
Youngest Displacement:	Pleistocene
Maximum Displacement:	> 610 m based on interpretation of gravity
Slip Rate:	No information
Recurrence Interval:	No information

Comment: Fault is well beyond the repository and fault displacement will not be a hazard. Peak acceleration is estimated to be 0.10 g at the surface at the refrence point. This estimate is based on a 7.1 (M_w) earthquake occurring 55 km from the refrence point.

Much of the information concerning the Belted Range fault is from reconnaissance field work or photogeologic interpretations.

Boomerang Point fault (BP)

Source of Information:	Simonds et al., 1995
Location:	Figure 1-2
Style of Faulting:	Dip Slip
Orientation of Fault:	Strike: North to northeast Dip: West
Maximum Fault Length:	5 km
Youngest Displacement:	No information
Maximum Displacement:	No information
Slip Rate:	No information
Recurrence Interval:	No information

Comment: Fault is beyond the repository and fault displacement will not be a hazard. Peak acceleration is estimated to be 0.56 g at the surface at the refrence point. This estimate is based on a 5.9 (M_w) earthquake occurring 2 km from the refrence point. The age of the most recent displacement of this fault cannot be determined because the fault does not offset post-tuff alluvium or colluvium. However, because this fault occurs in close proximity to faults of Quaternary age it is considered to be a Type I fault.

Type I Faults (cont'd)

Bow Ridge fault (BR)

Sources of Information:	Simonds et al., 1995; Piety, 1996
Location:	Figure 1-2
Style of Faulting:	Dip Slip or Oblique Slip Left-Lateral
Orientation of Fault:	Strike: North–South Dip: 69° W
Maximum Fault Length:	8 km (Simonds et al., 1995), 10 km (Piety, 1996)
Youngest Displacement:	Late Pleistocene
Maximum Displacement:	Variable along strike. Bedrock: 220 m (vertical separation of Topopah Spring tuff) Alluvium: 132 cm (cumulative)
Slip Rate:	0.016–0.018 mm/yr
Recurrence Interval:	10^4 to 10^5 yr

Comment: Fault is within the controlled area, but outside the repository perimeter. The Bow Ridge fault was intersected by the Exploration Studies Facilities (ESF) tunnel. The Bow Ridge fault creates a potential fault displacement hazard that needs to be evaluated. Given the maximum slip rate of 0.018 mm/yr and a 100 yr life for the ESF tunnel, an average of several mm of displacement would be expected over the required life of the tunnel. Peak acceleration is estimated to be 0.61 g at the surface at the refrence point. This estimate is based on a 6.1 (M_w) earthquake occurring 2.34 km from the refrence point.

Cane Spring fault (CS)

Sources of Information:	Nakata et al., 1982; Piety, 1996
Location:	Figure 1-1
Style of Faulting:	Oblique Slip Left-Lateral or Strike Slip Left-Lateral
Orientation of Fault:	Strike: Northeast Dip: No information
Maximum Fault Length:	14 km
Youngest Displacement:	Quaternary
Maximum Displacement:	No information
Slip Rate:	No information
Recurrence Interval:	No information

Comment: Fault is well beyond the repository and fault displacement will not be a hazard. Peak acceleration is estimated to be 0.13 g at the surface at the refrence point. This estimate is based on a 6.40 (M_w) earthquake occurring 29 km from the refrence point. Age of last displacement and amount of total displacement are poorly constrained.

Type I Faults (cont'd)

Carpetbag fault (CB)

Sources of Information:	Piety, 1996; Nakata et al., 1982
Location:	Figure 1-1
Style of Faulting:	Oblique Slip Right-Lateral
Orientation of Fault:	Strike: North to north-northwest Dip: East
Maximum Fault Length:	30 km
Youngest Displacement:	37 to 90 Ky (Knauss, 1981)
Maximum Displacement:	Bedrock: 600 m (vertical); Carr (1974) estimates there may be an equal or greater amount of right-lateral offset
Slip Rate:	No information
Recurrence Interval:	25,000 yr

Comment: Fault is well beyond the repository and fault displacement will not be a hazard. Peak acceleration is estimated to be 0.12 g at the surface at the refrence point. This estimate is based on a 6.4 (M_w) earthquake occurring 43 km from the refrence point. Pezzopane (1995) calculates a 6.5 (M_w) earthquake for a 30-km-long fault.

Crater Flat fault (CFF)

Sources of Information:	Simonds et al., 1995; Piety, 1996; Swadley et al., 1984
Location:	Figure 1-2
Style of Faulting:	Dip Slip or Oblique Slip Left-Lateral
Orientation of Fault:	Strike: North to north-northeast Dip: 70° W
Maximum Fault Length:	No information
Youngest Displacement:	Late Quaternary
Maximum Displacement:	No information
Slip Rate:	No information
Recurrence Interval:	No information

Comment: Fault is well beyond the repository and fault displacement will not be a hazard. Peak acceleration is estimated to be 0.54 g at the surface at the refrence point. This estimate is based on a 6.2 (M_w) earthquake occurring 10 km from the refrence point.

The CFF system consists of five faults (Piety, 1996) or two faults (Simonds et al., 1995). The fault characterized here is the eastern fault of Simonds et al. (1995) and fault S of Swadley et al. (1984). The other faults are described as the Simonds fault 10 (Figure 1-2) is fault T of Swadley et al. (1984); Simonds fault 11 (Figure 1-2) is the Black Cone fault of Piety (1996); Simonds fault 19 (Figure 1-2) is the West Lava fault of Piety (1996) and the southern part of Windy Wash fault is fault U of Swadley et al. (1984).

Type I Faults (cont'd)

Death Valley fault (DV)

Sources of Information:	Nakata et al., 1982; Piety, 1996
Location:	Figure 1-1
Style of Faulting:	Oblique Slip Right-Lateral
Orientation of Fault:	Strike: North-northwest Dip: 60° or steeper W
Maximum Fault Length:	61 km
Youngest Displacement:	Holocene
Maximum Displacement:	Vertical: 2 mm to 20 m Horizontal: 3.6 km
Slip Rate:	0.08–11.5 mm/yr
Recurrence Interval:	650 yr

Comment: Fault is well beyond the repository and fault displacement will not be a hazard. Peak acceleration is estimated to be 0.12 g at the surface at the refrence point. This estimate is based on a 7.2 (M_w) earthquake occurring 50 km from the refrence point. The maximum length of the Death Valley fault in the Piety (1996) coverage is 104 km and is located 43 km from the refrence point at the surface and would have an estimated peak acceleration of 0.12 g, based on a 7.4 (M_w) earthquake.

Pezzopane (1995) calculates a 7.4 (M_w) earthquake for a fault length of 100 km and a 7.4 (M_w) earthquake for the 288 km Death Valley–Furnace Creek–Fish Lake Valley fault.

Eleana Range fault (ER)

Source of Information:	Piety, 1996
Location:	Figure 1-1
Style of Faulting:	Dip Slip
Orientation of Fault:	Strike: Northeast to north-northeast Dip: East
Maximum Fault Length:	13 km
Youngest Displacement:	Late Pleistocene
Maximum Displacement:	No information
Slip Rate:	No information
Recurrence Interval:	No information

Comment: Fault is well beyond the repository and fault displacement will not be a hazard. Peak acceleration is estimated to be 0.1 g at the surface at the refrence point. This estimate is based on a 6.4 (M_w) earthquake occurring 37 km from the refrence point.

Type I Faults (cont'd)

Fatigue Wash fault (FW)

Source of Information:	Simonds et al., 1995
Location:	Figure 1-2
Style of Faulting:	Oblique Slip Left-Lateral
Orientation of Fault:	Strike: North-northeast to north-northwest Dip: 73° W
Maximum Fault Length:	33 km
Youngest Displacement:	Holocene
Maximum Displacement:	72 m
Slip Rate:	No information
Recurrence Interval:	No information

Comment: Fault is beyond the repository and fault displacement will not be a hazard. Peak acceleration is estimated to be 0.80 g at the surface at the refrence point. This estimate is based on a 7.7 (M_w) earthquake occurring 2 km from the refrence point. Pezzopane (1995) calculates a 6.5 (M_w) earthquake for a fault length of 17 km.

Furnace Creek fault (FC)

Sources of Information:	Nakata et al., 1982; Piety, 1996
Location:	Figure 1-1
Style of Faulting:	Oblique Slip Right-Lateral
Orientation of Fault:	Strike: Northwest Dip: No information
Maximum Fault Length:	123 km
Youngest Displacement:	Holocene
Maximum Displacement:	Horizontal 80 km
Slip Rate:	0.3–2.3 mm/yr (horizontal)
Recurrence Interval:	1,700 to 2,500 yr

Comment: Fault is well beyond the repository and fault displacement will not be a hazard. Peak acceleration is estimated to be 0.15 g at the surface at the refrence point. This estimate is based on a 7.5 (M_w) earthquake occurring 49 km from the refrence point. Piety (1996) lists the maximum length of this fault as 250 km. For this length, peak acceleration is estimated to 0.19 g at the surface at the refrence point. This estimate is based on a 7.9 (M_w) earthquake occurring 49 km from the refrence point. Pezzopane (1995) calculates a 7.9 (M_w) earthquake for the 288-km-long Death Valley–Furnace Creek–Fish Lake Valley fault.

Type I Faults (cont'd)

Ghost Dance fault (GD)

Sources of Information:	Simonds et al., 1995; Piety, 1996
Location:	Figure 1-2
Style of Faulting:	Dip Slip
Orientation of Fault:	Strike: North Dip: 50–89° W
Maximum Fault Length:	9 km
Youngest Displacement:	Quaternary: No direct evidence
Maximum Displacement:	30 m
Slip Rate:	No information
Recurrence Interval:	No information

Comment: The Ghost Dance fault occurs within the repository and therefore is a potential fault displacement hazard that needs to be evaluated. In Figure 1-2; the GD fault is linked to the AWF fault for a total length of 9 km. Peak acceleration is estimated to be 0.69 g at the surface at the refrence point. This estimate is based on a 6.2 (M_w) earthquake occurring 0.4 km from the refrence point. Pezzopane (1995) calculates a 5.6 (M_w) earthquake for the 3-km-long GD fault and a 6.1 (M_w) earthquake for the 7 km long GD–AWF.

Iron Ridge fault (IR)

Source of Information:	Simonds et al., 1995
Location:	Figure 1-2
Style of Faulting:	Dip Slip
Orientation of Fault:	Strike: North Dip: 68° W
Maximum Fault Length:	9 km
Youngest Displacement:	Quaternary
Maximum Displacement:	No information
Slip Rate:	No information
Recurrence Interval:	No information

Comment: Fault is well beyond the repository and fault displacement will not be a hazard. Peak acceleration is estimated to be 0.59 g at the surface at the refrence point. This estimate is based on a 6.2 (M_w) earthquake occurring 3 km from the refrence point. This fault is not listed in Piety (1996) or Pezzopane (1995).

Type I Faults (cont'd)

Kawich Range fault (KR)

Source of Information:	Piety, 1996
Location:	Figure 1-1
Style of Faulting:	Dip Slip
Orientation of Fault:	Strike: Variable northwest to northeast Dip: West
Maximum Fault Length:	84 km
Youngest Displacement:	Middle to Late Pleistocene
Maximum Displacement:	> 1,200 m
Slip Rate:	No information
Recurrence Interval:	No information

Comment: Fault is well beyond the repository and fault displacement will not be a hazard. Peak acceleration is estimated to be 0.11 g at the surface at the refrence point. This estimate is based on a 7.3 (M_w) earthquake occurring 57 km from the refrence point.

Keane Wonder fault (KW)

Sources of Information:	Nakata et al., 1982; Piety, 1996
Location:	Figure 1-1
Style of Faulting:	Dip Slip and/or Strike Slip Right-Lateral
Orientation of Fault:	Strike: Northwest Dip: 25° to 40° W
Maximum Fault Length:	33 km
Youngest Displacement:	Quaternary
Maximum Displacement:	5 km
Slip Rate:	No information
Recurrence Interval:	No information

Comment: Fault is well beyond the repository and fault displacement will not be a hazard. Peak acceleration is estimated to be 0.12 g at the surface at the refrence point. Peak acceleration is estimated to be 0.12 g at the surface at the refrence point. This estimate is based on a 6.8 (M_w) earthquake occurring 42 km from the refrence point.

Type I Faults (cont'd)

Midway Valley fault (MVF)

Source of Information:	Simonds et al., 1995
Location:	Figure 1-2
Style of Faulting:	Dip Slip
Orientation of Fault:	Strike: North Dip: West
Maximum Fault Length:	8 km
Youngest Displacement:	Quaternary
Maximum Displacement:	No information
Slip Rate:	No information
Recurrence Interval:	No information

Comment: Fault is well beyond repository and fault displacement will not be a hazard. Peak acceleration is estimated to be 0.51 g at the surface at the refrence point. This estimate is based on a 5.9 (M_w) earthquake occurring 3 km from the refrence point. Age of last displacement and amount of total displacement is poorly constrained. This fault is not listed in Piety (1995) or Pezzopane (1995).

Mine Mountain fault (MM)

Sources of Information:	Nakata et al., 1982; Piety, 1996
Location:	Figure 1-1
Style of Faulting:	Oblique Slip Left-Lateral
Orientation of Fault:	Strike: Northeast Dip: Southeast
Maximum Fault Length:	5.6 km
Youngest Displacement:	Quaternary
Maximum Displacement:	1 km left-lateral slip
Slip Rate:	0.07–0.90 mm/yr
Recurrence Interval:	No information

Comment: Fault is well beyond the repository and fault displacement will not be a hazard. Peak acceleration is estimated to be 0.12 g at the surface at the refrence point. This estimate is based on a 6.0 (M_w) earthquake, for the maximum fault length, occurring 24 km from the refrence point. Pezzopane (1995) calculates a 6.7 (M_w) earthquake for a 27-km-long fault.

Type I Faults (cont'd)

Oasis Valley faults (OSV)

Source of Information:	Nakata et al., 1982; Piety, 1996
Location:	Figure 1-1
Style of Faulting:	Dip Slip
Orientation of Fault:	Strike: North-northeast Dip: West
Maximum Fault Length:	16 km
Youngest Displacement:	Pleistocene
Maximum Displacement:	No information
Slip Rate:	0.001–0.005 mm/yr
Recurrence Interval:	No information

Comment: Piety (1996) lists two faults in the description of the Oasis Valley faults. The western fault is 6 km from the eastern fault. Faults are well beyond the repository and fault displacement will not be a hazard. Peak acceleration on the eastern fault is estimated to be 0.18 g at the surface at the refrence point. This estimate is based on a 6.5 (M_w) earthquake occurring 24 km from the refrence point. A western fault is 30 km away, 7 km long, with an estimated 0.09 g peak acceleration at the repository. This fault is classified as Type III.

Pahrump fault (PRP)

Source of Information:	Nakata et al., 1982; Piety, 1996
Location:	Figure 1-1
Style of Faulting:	Oblique Slip Right-Lateral or Strike Slip Right-Lateral
Orientation of Fault:	Strike: Northwest-northeast Dip: West
Maximum Fault Length:	130 km
Youngest Displacement:	Late Pleistocene to Holocene
Maximum Displacement:	Vertical: 300 m Horizontal: 16–19 km
Slip Rate:	No information
Recurrence Interval:	No information

Comment: Fault is well beyond the repository and fault displacement will not be a hazard. Peak acceleration is estimated to be 0.10 g at the surface at the refrence point. This estimate is based on a 6.7 (M_w) earthquake occurring 70 km from the refrence point. Pezzopane (1995) calculates a 7.2 (M_w) earthquake for the 70 km Pahrump–Stewart Valley fault.

Type I Faults (cont'd)

Paintbrush Canyon fault (PBC)

Sources of Information:	Simonds et al., 1995; Piety, 1996
Location:	Figure 1-2
Style of Faulting:	Dip Slip
Orientation of Fault:	Strike: North-northeast Dip: 71° W
Maximum Fault Length:	24 km (Simonds, et al., 1995) 30 km (Piety, 1996)
Youngest Displacement:	Late Quaternary
Maximum Displacement:	500 m
Slip Rate:	0.0083 mm/yr (Quaternary)
Recurrence Interval:	117,000 to 140,000 yr

Comment: Fault is beyond the repository and fault displacement will not be a hazard. Peak acceleration is estimated to be 0.66 g at the surface at the refrence point. This estimate is based on a 6.7 (M_w) earthquake occurring 4 km from the refrence point.

Plutonium Valley–North Halfpint Range faults (PVNH)

Source of Information:	Nakata et al., 1982; Piety, 1996
Location:	Figure 1-1
Style of Faulting:	Dip Slip
Orientation of Fault:	Strike: North-northwest Dip: Dominantly to East
Maximum Fault Length:	26 km
Youngest Displacement:	Quaternary
Maximum Displacement:	No information
Slip Rate:	No information
Recurrence Interval:	No information

Comment: Fault is beyond the repository and fault displacement will not be a hazard. Peak acceleration is estimated to be 0.10 g at the surface at the refrence point. This estimate is based on a 6.7 (M_w) earthquake occurring 46 km from the refrence point.

Type I Faults (cont'd)

Rock Valley fault (RV)

Sources of Information:	Nakata et al., 1982; Piety, 1996
Location:	Figure 1-1
Style of Faulting:	Strike Slip Left-Lateral or Oblique Slip Left-Lateral
Orientation of Fault:	Strike: Northeast Dip: 70° SE
Maximum Fault Length:	43 km
Youngest Displacement:	Pleistocene; Holocene along southwest extension
Maximum Displacement:	A few kilometers total lateral displacement
Slip Rate:	0.003–0.01 mm/yr
Recurrence Interval:	No information

Comment: Fault is beyond the repository and fault displacement will not be a hazard. Peak acceleration is estimated to be 0.23 g at the surface at the refrence point. This estimate is based on a 7.0 (M_w) earthquake occurring 25 km from the refrence point. Based on fault length of 65 km, a 7.2 (M_w) earthquake with an associated peak acceleration of 0.25 g is estimated. Piety (1996) links the Rock Valley fault extension to the southwest with the 43-km main Rock Valley fault for a total length of 65 km.

Rocket Wash–Beatty Wash fault (RWBW)

Source of Information:	Piety, 1996
Location:	Figure 1-1
Style of Faulting:	Dip Slip
Orientation of Fault:	Strike: North to north-northeast Dip: West
Maximum Fault Length:	17 km
Youngest Displacement:	Quaternary
Maximum Displacement:	No information
Slip Rate:	No information
Recurrence Interval:	No information

Comment: Fault is beyond the repository and fault displacement will not be a hazard. Peak acceleration is estimated to be 0.23 g at the surface at the refrence point. This estimate is based on a 6.5 (M_w) earthquake occurring 19 km from the refrence point.

Type I Faults (cont'd)

Sarcobatus Flat fault (SF)

Source of Information:	Piety, 1996
Location:	Figure 1-1
Style of Faulting:	Dip Slip
Orientation of Fault:	Strike: North-northwest Dip: West
Maximum Fault Length:	51 km
Youngest Displacement:	Quaternary
Maximum Displacement:	No information
Slip Rate:	No information
Recurrence Interval:	No information

Comment: Fault is beyond the repository and fault displacement will not be a hazard. Peak acceleration is estimated to be 0.10 g at the surface at the refrence point. This estimate is based on a 7.1 (M_w) earthquake occurring 52 km from the refrence point.

Simonds Number 1 fault

Sources of Information:	Simonds et al., 1995; Frizzell and Shulters, 1990
Location:	Figure 1-2
Style of Faulting:	Dip Slip
Orientation of Fault:	Strike: North-northwest Dip: West
Maximum Fault Length:	3 km
Youngest Displacement:	No information
Maximum Displacement:	No information
Slip Rate:	No information
Recurrence Interval:	No information

Comment: Fault is beyond the repository and fault displacement will not be a hazard. The age of the most recent displacement of this fault cannot be determined because the fault does not offset post-tuff alluvium or colluvium. However, because this fault occurs in close proximity to faults of Quaternary age it is considered to be a Type I fault. Peak acceleration is estimated to be 0.32 g at the surface at the refrence point. This estimate is based on a 5.6 (M_w) earthquake occurring 7 km from the refrence point.

Type I Faults (cont'd)

Simonds Number 2 fault

Source of Information:	Simonds et al., 1995
Location:	Figure 1-2
Style of Faulting:	Dip Slip
Orientation of Fault:	Strike: North Dip: West
Maximum Fault Length:	7 km
Youngest Displacement:	No information
Maximum Displacement:	No information
Slip Rate:	No information
Recurrence Interval:	No information

Comment: Fault is beyond the repository and fault displacement will not be a hazard. The age of the most recent displacement of this fault cannot be determined because the fault does not offset post-tuff alluvium or colluvium. However, because this fault occurs in close proximity to faults of Quaternary age it is considered to be a Type I fault. Peak acceleration is estimated to be 0.44 g at the surface at the refrence point. This estimate is based on a 7.28 (M_w) earthquake, for the maximum fault length, occurring 6 km from the refrence point.

Simonds Number 3 fault

Sources of Information:	Simonds et al., 1995; Frizzell and Shulters, 1990
Location:	Figure 1-2
Style of Faulting:	Dip Slip
Orientation of Fault:	Strike: North-northwest Dip: West
Maximum Fault Length:	5 km
Youngest Displacement:	No information
Maximum Displacement:	No information
Slip Rate:	No information
Recurrence Interval:	No information

Comment: Fault is beyond the repository and fault displacement will not be a hazard. The age of the most recent displacement of this fault cannot be determined because the fault does not offset post-tuff alluvium or colluvium. However, because this fault occurs in close proximity to faults of Quaternary age it is considered to be a Type I fault. Peak acceleration is estimated to be 0.44 g at the surface at the refrence point. This estimate is based on a 5.9 (M_w) earthquake occurring 5 km from the refrence point.

Type I Faults (cont'd)

Simonds Number 4 fault

Sources of Information:	Simonds et al., 1995; Frizzell and Shulters, 1990
Location:	Figure 1-2
Style of Faulting:	Dip Slip
Orientation of Fault:	Strike: North-northwest Dip: East
Maximum Fault Length:	5 km
Youngest Displacement:	No information
Maximum Displacement:	No information
Slip Rate:	No information
Recurrence Interval:	No information

Comment: Fault is beyond the repository and fault displacement will not be a hazard. The age of the most recent displacement of this fault cannot be determined because the fault does not offset post-tuff alluvium or colluvium. However, because this fault occurs in close proximity to faults of Quaternary age it is considered to be a Type I fault. Peak acceleration is estimated to be 0.45 g at the surface at the refrence point. This estimate is based on a 5.9 (M_w) earthquake occurring 5 km from the refrence point.

Simonds Number 5 fault

Sources of Information:	Simonds et al., 1995; Frizzell and Shulters, 1990
Location:	Figure 1-2
Style of Faulting:	Dip Slip
Orientation of Fault:	Strike: Northwest Dip: Southwest
Maximum Fault Length:	5 km
Youngest Displacement:	No information
Maximum Displacement:	No information
Slip Rate:	No information
Recurrence Interval:	No information

Comment: Fault is beyond the repository and fault displacement will not be a hazard. The age of the most recent displacement of this fault cannot be determined because the fault does not offset post-tuff alluvium or colluvium. However, because this fault occurs in close proximity to faults of Quaternary age it is considered to be a Type I fault. Peak acceleration is estimated to be 0.42 g at the surface at the refrence point. This estimate is based on a 5.9 (M_w) earthquake occurring 6 km from the refrence point.

Type I Faults (cont'd)

Simonds Number 6 fault

Sources of Information: Simonds et al., 1995; Frizzell and Shulters, 1990

Comment: Simonds Number 6 fault was considered a separate fault in McKague (1996, Figure 8). In this report it is considered the northern extension of Windy Wash fault and is not shown on Figure 1-2.

Simonds Number 7 fault

Sources of Information:	Simonds et al., 1995; Frizzell and Shulters, 1990
Location:	Figure 1-2
Style of Faulting:	Dip Slip
Orientation of Fault:	Strike: North Dip: East
Maximum Fault Length:	5 km
Youngest Displacement:	No information
Maximum Displacement:	No information
Slip Rate:	No information
Recurrence Interval:	No information

Comment: Fault is beyond the repository and fault displacement will not be a hazard. Peak acceleration is estimated to be 0.32 g at the surface at the refrence point. This estimate is based on a 5.9 (M_w) earthquake occurring 8 km from the refrence point. The age of the most recent displacement of this fault cannot be determined because the fault does not offset post-tuff alluvium or colluvium. However, because this fault occurs in close proximity to faults of Quaternary age it is considered to be a Type I fault.

Type I Faults (cont'd)

Simonds Number 8 fault

Sources of Information:	Simonds et al., 1995; Frizzell and Shulters, 1990
Location:	Figure 1-2
Style of Faulting:	Dip Slip
Orientation of Fault:	Strike: North Dip: West
Maximum Fault Length:	7 km
Youngest Displacement:	No information
Maximum Displacement:	No information
Slip Rate:	No information
Recurrence Interval:	No information

Comment: Fault is beyond the repository and fault displacement will not be a hazard. Peak acceleration is estimated to be 0.36 g at the surface at the refrence point. This estimate is based on a 6.1 (M_w) earthquake occurring 9 km from the refrence point. The age of the most recent displacement of this fault cannot be determined because the fault does not offset post-tuff alluvium or colluvium. However, because this fault occurs in close proximity to faults of Quaternary age it is considered to be a Type I fault.

Simonds Number 9 fault

Sources of Information:	Simonds et al., 1995; Frizzell and Shulters, 1990
Location:	Figure 1-2
Style of Faulting:	Dip Slip
Orientation of Fault:	Strike: North Dip: West
Maximum Fault Length:	4 km
Youngest Displacement:	No information
Maximum Displacement:	No information
Slip Rate:	No information
Recurrence Interval:	No information

Comment: Fault is beyond the repository and fault displacement will not be a hazard. Peak acceleration is estimated to be 0.28 g at the surface at the refrence point. This estimate is based on a 5.8 (M_w) earthquake occurring 9 km from the refrence point. The age of the most recent displacement of this fault cannot be determined because the fault does not offset post-tuff alluvium or colluvium. However, because this fault occurs in close proximity to faults of Quaternary age it is considered to be a Type I fault.

Type I Faults (cont'd)

Simonds Number 10 fault

Sources of Information:	Simonds et al., 1995; Frizzell and Shulters, 1990
Location:	Figure 1-2
Style of Faulting:	Dip Slip
Orientation of Fault:	Strike: North Dip: West
Maximum Fault Length:	5 km
Youngest Displacement:	No information
Maximum Displacement:	No information
Slip Rate:	No information
Recurrence Interval:	No information

Comment: Fault is beyond the repository and fault displacement will not be a hazard. Peak acceleration is estimated to be 0.30 g at the surface at the refrence point. This estimate is based on a 5.9 (M_w) earthquake occurring 9 km from the refrence point. The age of the most recent displacement of this fault cannot be determined because the fault does not offset post-tuff alluvium or colluvium. However, because this fault occurs in close proximity to faults of Quaternary age it is considered to be a Type I fault. This is fault T of Swadley et al. (1984).

Simonds Number 11 fault

Source of Information:	Simonds et al., 1995
Location:	Figure 1-2
Style of Faulting:	Dip Slip and/or Oblique Slip Left-Lateral
Orientation of Fault:	Strike: North to north-northeast Dip: West
Maximum Fault Length:	7 km
Youngest Displacement:	No information
Maximum Displacement:	No information
Slip Rate:	No information
Recurrence Interval:	No information

Comment: Fault is beyond the repository and fault displacement will not be a hazard. Peak acceleration is estimated to be 0.43 g at the surface at the refrence point. This estimate is based on a 6.0 (M_w) earthquake occurring 6 km from the refrence point. The age of the most recent displacement of this fault cannot be determined because the fault does not offset post-tuff alluvium or colluvium. However, because this fault occurs in close proximity to faults of Quaternary age it is considered to be a Type I fault. This is the Black Cone fault of Piety (1996).

Type I Faults (cont'd)

Simonds Number 12 fault

Source of Information:	Simonds et al., 1995
Location:	Figure 1-2
Style of Faulting:	Dip Slip
Orientation of Fault:	Strike: North to northwest Dip: West
Maximum Fault L ngth:	8 km
Youngest Displacement:	Quaternary
Maximum Displacement:	No information
Slip Rate:	No information
Recurrence Interval:	No information

Comment: Fault is beyond the repository and fault displacement will not be a hazard. Peak acceleration is estimated to be 0.47 g at the surface at the refrence point. This estimate is based on a 6.1 (M_w) earthquake occurring 6 km from the refrence point.

Simonds Number 13 fault

Source of Information:	Simonds et al., 1995

Comment: Simonds Number 13 fault (McKague, 1996, Figure 8) is the Boomerang Point fault.

Simonds Number 14 fault

Source of Information:	Simonds et al., 1995
Location:	Figure 1-2
Style of Faulting:	Dip Slip
Orientation of Fault:	Strike: North Dip: Vertical
Maximum Fault Length:	8 km
Youngest Displacement:	Quaternary
Maximum Displacement:	No information
Slip Rate:	No information
Recurrence Interval:	No information

Comment: Fault is beyond the repository and fault displacement will not be a hazard. Peak acceleration is estimated to be 0.64 g at the surface at the refrence point. This estimate is based on a 6.1 (M_w) earthquake occurring 2 km from the refrence point.

Type I Faults (cont'd)

Simonds Number 15 fault

Source of Information:	Simonds et al., 1995
Location:	Figure 1-2
Style of Faulting:	Dip Slip
Orientation of Fault:	Strike: North to northwest Dip: East and West
Maximum Fault Length:	4 km
Youngest Displacement:	No information
Maximum Displacement:	No information
Slip Rate:	No information
Recurrence Interval:	No information

Comment: Fault is beyond the repository and fault displacement will not be a hazard. Peak acceleration is estimated to be 0.47 g at the surface at the refrence point. This estimate is based on a 5.8 (M_w) earthquake occurring 4 km from the refrence point. The age of the most recent displacement of this fault cannot be determined because the fault does not offset post-tuff alluvium or colluvium. However, because this fault occurs in close proximity to faults of Quaternary age it is considered to be a Type I fault.

Simonds Number 16 fault

Source of Information:	Simonds et al., 1995
Location:	Figure 1-2
Style of Faulting:	Dip Slip
Orientation of Fault:	Strike: North Dip: Predominantly west at southern end of fault and east at northern end of fault
Maximum Fault Length:	4 km
Youngest Displacement:	No information
Maximum Displacement:	No information
Slip Rate:	No information
Recurrence Interval:	No information

Comment: Fault is beyond the repository and fault displacement will not be a hazard. Peak acceleration is estimated to be 0.34 g at the surface at the refrence point. This estimate is based on a 5.8 (M_w) earthquake occurring 7 km from the refrence point. The age of the most recent displacement of this fault cannot be determined because the fault does not offset post-tuff alluvium or colluvium. However, because this fault occurs in close proximity to faults of Quaternary age it is considered to be a Type I fault.

Type I Faults (cont'd)

Simonds Number 17 fault

Source of Information:	Simonds et al., 1995
Location:	Figure 1-2
Style of Faulting:	Dip Slip
Orientation of Fault:	Strike: North-northeast Dip: West
Maximum Fault Length:	10 km
Youngest Displacement:	No information
Maximum Displacement:	No information
Slip Rate:	No information
Recurrence Interval:	No information

Comment: Fault is beyond the repository and fault displacement will not be a hazard. Peak acceleration is estimated to be 0.40 g at the surface at the refrence point. This estimate is based on a 6.2 (M_w) earthquake occurring 8 km from the refrence point. The age of the most recent displacement of this fault cannot be determined because the fault does not offset post-tuff alluvium or colluvium. However, because this fault occurs in close proximity to faults of Quaternary age it is considered to be a Type I fault.

Simonds Number 18 fault

Sources of Information:	Simonds et al., 1995; Frizzell and Shulters, 1990
Location:	Figure 1-2
Style of Faulting:	Dip Slip
Orientation of Fault:	Strike: North-northeast Dip: East
Maximum Fault Length:	3 km
Youngest Displacement:	No information
Maximum Displacement:	No information
Slip Rate:	No information
Recurrence Interval:	No information

Comment: Fault is beyond the repository and fault displacement will not be a hazard. Peak acceleration is estimated to be 0.19 g at the surface at the refrence point. This estimate is based on a 5.6 (M_w) earthquake occurring 13 km from the refrence point. The age of the most recent displacement of this fault cannot be determined because the fault does not offset post-tuff alluvium or colluvium. However, because this fault occurs in close proximity to faults of Quaternary age it is considered to be a Type I fault.

Type I Faults (cont'd)

Simonds Number 19 fault

Sources of Information:	Simonds et al., 1995; Frizzell and Shulters, 1990
Location:	Figure 1-2
Style of Faulting:	Dip Slip
Orientation of Fault:	Strike: North-northeast Dip: West
Maximum Fault Length:	8 km
Youngest Displacement:	Quaternary
Maximum Displacement:	No information
Slip Rate:	No information
Recurrence Interval:	No information

Comment: Fault is beyond the repository and fault displacement will not be a hazard. Peak acceleration is estimated to be 0.39 g at the surface at the refrence point. This estimate is based on a 6.1 (M_w) earthquake occurring 8 km from the refrence point. This is the West Lava fault of Piety (1996).

Solitario Canyon fault (SC)

Sources of Information:	Simonds et al., 1995; Piety, 1996
Location:	Figure 1-2
Style of Faulting:	Dip Slip or Oblique Slip Left-Lateral
Orientation of Fault:	Strike: North-northeast Dip: West
Maximum Fault Length:	19 km
Youngest Displacement:	Pleistocene
Maximum Displacement:	1 km (vertical at south end)
Slip Rate:	0.03–0.06 mm/yr
Recurrence Interval:	No information

Comment: The Solitario Canyon fault is just beyond the western boundary of the repository. Direct disruption of the repository by fault displacement on the Solitario Canyon fault appears unlikely. However, a splay off the fault crosses into the repositoy from the west and should be evaluated. Small coseismic movement on nearby faults could produce small displacements within the repository. Peak acceleration is estimated to be 0.76 g at the surface at the refrence point. This estimate is based on a 6.6 (M_w) earthquake occurring 1 km from the refrence point.

Type I Faults (cont'd)

Stagecoach Road fault (SCR)

Sources of Information:	Simonds et al., 1995; Piety, 1996
Location:	Figure 1-2
Style of Faulting:	Dip Slip and/or Oblique Slip Left-Lateral
Orientation of Fault:	Strike: Northeast Dip: 73° W
Maximum Fault Length:	8 km
Youngest Displacement:	Pleistocene
Maximum Displacement:	1 km
Slip Rate:	0.003 mm/yr
Recurrence Interval:	No information

Comment: Fault is well beyond repository and fault displacement will not be a hazard. Peak acceleration is estimated to be 0.30 g at the surface at the refrence point. This estimate is based on a 6.1 (M_w) earthquake occurring 11 km from the refrence point.

Note: The 10 km cumulative displacement listed in Piety (1996) is incorrect. Values in Scott (1990) are 0.67×10^6 mm (670 m) for the time period 13--11.5 Ma and 0.33×10^6 mm (330 m) for the time period 11.5 Ma to present.

Tolicha Peak fault (TOL)

Source of Information:	Nakata et al., 1982; Piety, 1996
Location:	Figure 1-1
Style of Faulting:	Dip Slip and Oblique Slip Right-Lateral
Orientation of Fault:	Strike: North-northwest Dip: Southwest
Maximum Fault Length:	22 km
Youngest Displacement:	Quaternary
Maximum Displacement:	No information
Slip Rate:	No information
Recurrence Interval:	No information

Comment: Fault is well beyond the repository and fault displacement will not be a hazard. Peak acceleration is estimated to be 0.10 g at the surface at the refrence point. This estimate is based on a 6.6 (M_w) earthquake occurring 42 km from the refrence point.

Type I Faults (cont'd)

Wahmonie fault (WAH)

Source of Information:	Nakata et al., 1982; Piety, 1996
Location:	Figure 1-1
Style of Faulting:	Dip Slip
Orientation of Fault:	Strike: North to northeast Dip: Northwest
Maximum Fault Length:	15 km
Youngest Displacement:	Pleistocene
Maximum Displacement:	No information
Slip Rate:	No information
Recurrence Interval:	No information

Comment: Fault is well beyond the repository and fault displacement will not be a hazard. Peak acceleration is estimated to be 0.19 g at the surface at the refrence point. This estimate is based on a 6.4 (M_w) earthquake occurring 22 km from the refrence point.

West Spring Mountain fault (WSM)

Source of Information:	Piety, 1996
Location:	Figure 1-1
Style of Faulting:	Dip Slip
Orientation of Fault:	Strike: Northwest to north-northeast Dip: West
Maximum Fault Length:	60 km
Youngest Displacement:	Pleistocene
Maximum Displacement:	3,500 m
Slip Rate:	0.06 mm/yr (vertical)
Recurrence Interval:	No information

Comment: Fault is well beyond the repository and fault displacement will not be a hazard. Peak acceleration is estimated to be 0.11 g at the surface at the refrence point. This estimate is based on a 7.1 (M_w) earthquake occurring 53 km from the refrence point.

Type I Faults (cont'd)

Windy Wash fault (WW)

Sources of Information:	Simonds et al., 1995; Piety, 1996
Location:	Figure 1-2
Style of Faulting:	Dip Slip
Orientation of Fault:	Strike: North Dip: 63° W
Maximum Fault Length:	28 km
Youngest Displacement:	Late Pleistocene or Holocene
Maximum Displacement:	> 500 m (Simonds et al., 1995); 30 m (Piety, 1996)
Slip Rate:	0.001 to 0.03 mm/yr
Recurrence Interval:	75,000 yr

Comment: Fault is well beyond the repository and fault displacement will not be a hazard. Peak acceleration is estimated to be 0.69 g at the surface at the refrence point. This estimate is based on a 6.8 (M_w) earthquake occurring 4 km from the refrence point. Southern part of WW fault is fault U of Swadley et al. (1984). Length is based on connecting several fault segments on Simon et al., 1995 map. Simon et al., (1995) and Piety (1996) have lengths of 19.5 km and 14 km, respectively.

Yucca fault (YC)

Sources of Information:	Nakata et al., 1982; Piety, 1996
Location:	Figure 1-1
Style of Faulting:	Dip Slip
Orientation of Fault:	North
Maximum Fault Length:	31 km
Youngest Displacement:	Holocene
Maximum Displacement:	Vertical: $\geq$ 200 m in Tertiary tuffs Horizontal: may equal or exceed vertical
Slip Rate:	No information
Recurrence Interval:	No information

Comment: Fault is well beyond the repository and fault displacement will not be a hazard. Peak acceleration is estimated to be 0.10 g at the surface at the refrence point. This estimate is based on a 6.8 (M_w) earthquake occurring 43 km from the refrence point.

Type I Faults (cont'd)

Yucca Lake fault (YCL)

Source of Information:	Nakata et al. 1982; Piety, 1996
Location:	Figure 1-1
Style of Faulting:	Dip Slip
Orientation of Fault:	Strike: North-northwest Dip: Northeast
Maximum Fault Length:	17 km
Youngest Displacement:	Pleistocene, possibly Holocene
Maximum Displacement:	610 m
Slip Rate:	No information
Recurrence Interval:	No information

Comment: Fault is well beyond the repository and fault displacement will not be a hazard. Peak acceleration is estimated to be 0.11 g at the surface at the refrence point. This estimate is based on a 6.5 (M_w) earthquake occurring 36 km from the refrence point.

Type II Fault

Beatty Scarp fault (BS)

Sources of Information:	Nakata et al., 1982; Piety, 1996
Location:	Figure 1-1
Style of Faulting:	Scarp has been interpreted as both a dip slip fault and an erosional feature
Orientation of Fault:	Strike: N 40° W to N 30° E Dip: West
Maximum Fault Length:	7.3 km, 8–10 km with a possible 15-km section concealed beneath alluvium
Youngest Displacement:	Quaternary, possibly Holocene
Maximum Displacement:	No information
Slip Rate:	No information
Recurrence Interval:	No information

Comment: Fault is well beyond the repository and fault displacement will not be a hazard. Peak acceleration is estimated to be 0.11 g at the surface at the refrence point. This estimate is based on a 6.1 (M_w) earthquake occurring 25 km from the refrence point. Given the uncertainty of the origin and the lack of detailed information this fault is considered to be a Type II fault. See discussion on page 2-4.

Type III Faults

Pagany fault (PWF)

Sources of Information:	Simonds et al., 1995; Piety, 1996
Location:	Figure 1-2
Style of Faulting:	Dip Slip
Orientation of Fault:	Strike: Northwest Dip: Vertical
Maximum Fault Length:	4 km
Youngest Displacement:	Weak evidence of Quaternary displacement
Maximum Displacement:	No information
Slip Rate:	No information
Recurrence Interval:	No information

Comment: Fault is beyond the repository and fault displacement will not be a hazard. Peak acceleration is estimated to be 0.46 g at the surface at the refrence point. This estimate is based on a 5.8 (M_w) earthquake occurring 2.6 km from the refrence point.

The age of this northwest-trending fault is poorly constrained, with weak evidence of Quaternary displacement. In addition, the orientation of the fault in the modern *in situ* stress field suggests a low tendency for slip along the fault. With the large number of faults in the YMR that are more suitabiy oriented for slip it is highly unlikely that this fault would slip. This is probably reflected by the poorly defined nature of this fault in the Quaternary alluvium and colluvium.

Sever Wash fault (SW)

Sources of Information:	Simonds et al., 1995; Piety, 1996
Location:	Figure 1-2
Style of Faulting:	Strike Slip
Orientation of Fault:	Strike: Northwest Dip: Vertical
Maximum Fault Length:	4.2 km
Youngest Displacement:	No evidence of Quaternary displacement
Maximum Displacement:	610 m
Slip Rate:	No information
Recurrence Interval:	No information

Comment: Fault is beyond the repository and fault displacement will not be a hazard. Peak acceleration is estimated to be 0.51 g at the surface at the refrence point. This estimate is based on a 5.8 (M_w) earthquake occurring 3 km from the refrence point.

Although the age of this northwest-trending fault is poorly constrained, there is no evidence of Quaternary displacement. In addition, the orientation of the fault in the modern *in situ* stress field suggests a low tendency for slip along the fault. With the large number of faults in the YMR that are more suitably oriented for slip it is highly unlikely that this these fault would slip. This is probably reflected by the poorly defined nature of this fault in the Quaternary alluvium and colluvium.

Type III Faults (cont'd)

Yucca Wash fault (YWF)

Source of Information:	Simonds et al., 1996; Piety, 1996
Location:	Figure 1-2
Style of Faulting:	Strike Slip Right-Lateral
Orientation of Fault:	Strike: Northwest Dip: Vertical
Maximum Fault Length:	7 km
Youngest Displacement:	No evidence of Quaternary movement
Maximum Displacement:	No information
Slip Rate:	No information
Recurrence Interval:	No information

Comment: Fault is beyond the repository and fault displacement will not be a hazard. Peak acceleration is estimated to be 0.49 g at the surface at the refrence point. This estimate is based on a 6.0 (M_w) earthquake occurring 5 km from the refrence point. Pezzopane (1995) calculates a 6.2 (M_w) earthquake for a 9-km-long fault.

Although the age of this northwest-trending fault is poorly constrained, there is no evidence of Quaternary displacement. In addition, the orientation of the fault in the modern *in situ* stress field suggests a low tendency for slip along the fault. With the large number of faults in the YMR that are more suitably oriented for slip it is highly unlikely that this fault would slip. This is probably reflected by the poorly defined nature of this fault in the Quaternary alluvium and colluvium.

REFERENCES
APPENDIX A

Campbell, K.W. 1987. Predicting strong ground motion in Utah. *Evaluation of Regional and Urban Earthquakes and Risk in Utah*. W.W. Hays and P.L. Gori, eds. U.S. Geological Survey Professional Paper 87-585II, L1-L90. Washington, D.C.

Carr, W.J. 1974. *Summary of Tectonic and Structural Evidence for Stress Orientation at the Nevada Test Site*. U.S. Geological Survey Open File Report 74-176. Reston, VA.

Donovan, D.E. 1991. *Neotectonics of the Southern Amargosa Desert, Nye County, Nevada, and Inyo County, California*. M.S Thesis. Reno, NV: University of Nevada.

Ferrill, D.A., G.L. Stirewalt, D.B. Henderson, J.A. Stamatakos, A.P. Morris, B.P. Wernicke, and K.H. Spivey. 1995. *Faulting in the Yucca Mountain Region: Critical Review and Analyses of Tectonic Data from the Central Basin and Range*. CNWRA 95-017. San Antonio, TX: Center for Nuclear Waste Regulatory Analyses.

Frizzell, V.A. Jr., and J. Shulters. 1990. *Geologic Map of the Nevada Test Site, Southern Nevada*. U.S. Geological Survey Miscellaneous Investigations Series, Map I-2046, Scale 1:100,000. Denver, CO.

Klinger, R.E., and L.W. Anderson. 1994. Topographic profiles and their implications for late Quaternary activity on the Bare Mountain fault, Nye County, Nevada. *Geological Society of America Abstracts with Programs 26(2)*.

Knauss, K.G. 1981. *Dating Fault Associated Quaternary Material from the Nevada Test Site Using Uranium—Series Methods*. UCRL-53231. Livermore, CA: Lawrence Livermore National Laboratory.

McKague, H.L. 1996. *Identification of Type II Faults in the Yucca Mountain Area*. Letter Report. San Antonio, TX: Center for Nuclear Waste Regulatory Analyses.

Monsen, S.A., M.D. Carr, M.C. Reheis, and P.P. Orkild. 1992. *Geologic Map of Bare Mountain, Nye County, Nevada*. U.S. Geological Survey Miscellaneous Investigations Series, Map I-2201, Scale 1:24,000. Denver, CO.

Nakata, J.K., C.M. Wentworth, and M.N. Machette. 1982. *Quaternary Fault Maps of the Basin and Range and Rio Grande Rift Provinces, Western United States*. Scale 1:2,500,000. U.S. Geological Survey Open File Report 82-579. Denver, CO.

Pezzopane, D.K. 1995. *Preliminary Table of Characteristics of Known and Suspected Quaternary Fault in the Yucca Mountain Area*. Administrative Report. U.S. Geological Survey. Denver, CO.

Piety, L.A. 1996. *Compilation of Known and Suspected Quaternary Faults Within 100 km of Yucca Mountain*. Scale 1:250,000. U.S. Geological Survey Open File Report 94-112 (Draft). Denver, CO.

Reheis, M.C. 1988. Preliminary study of Quaternary faulting on the east side of Bare Mountain, Nye County, Nevada. Geologic and hydrologic investigations of a potential nuclear waste disposal site at Yucca Mountain, southern Nevada. M.D. Carr and J.C. Yount, eds. *U.S. Geological Survey Bulletin* 1790: 103–111.

Scott, R.B. 1990. Tectonic setting of Yucca Mountain, southwest Nevada. Basin and range extensional tectonics near the latitude of Las Vegas, Nevada. B.P. Wernicke, ed. *Geological Society of America Memoir 176*: 251–282

Simonds, W.F., J.W. Whitney, E. Fox, A. Ramelli, J.C. Yount, M.D. Carr, C.D. Menges, R. Dickerson, and R.J. Scott. 1995. *Map of Fault Activity of the Yucca Mountain Area, Nye County, Nevada*. U.S. Geological Survey Miscellaneous Investigations Series, Map 1-2520. Scale 1:24,000. Denver, CO.

Swadley, W.C., D.L. Hoover, and J.N. Rosholt. 1984. *Preliminary Report on Late Cenozoic Faulting and Stratigraphy in the Vicinity of Yucca Mountain, Nye County, Nevada*. Scale: 1:62,500. U.S. Geological Survey Open-File Report 84-788. Denver, CO.

Wells, D.L., and K.J. Coppersmith. 1994. New empirical relationships among magnitude, rupture length, rupture width, rupture area, and surface displacement. *Bulletin of the Seismological Society of America* 84: 974–1,002.

APPENDIX B

LIST OF FAULTS AND ABBREVIATIONS FROM PIETY (1996) AND SIMONDS ET AL.(1995)

Fault Name	Fault Abbreviation
Ash Hill Fault	AH
Airport Lake Fault	AIR
Ash Meadows Fault	AM
Amargosa River Fault	AR
Area Three Fault	AT
Bonnie Claire Fault	BC
Boundary Fault	BD
Badger Wash Faults	BDG
Buried Hills Fault	BH
Belted Range Fault	BLR
Bare Mountain Fault	BM
Boomerang Point Fault	BP
Bow Ridge Fault	BR
Beatty Scarp	BS
Bullfrog Hills Faults	BUL
Cactus Springs Fault	CAC
Carpetbag Fault	CB
Cactus Flat Fault	CF
Crater Flat Fault*	CFF
Cactus Flat—Mellan Fault	CFML
Crossgrain Valley Fault	CGV
Chert Ridge Faults	CHR
Chicago Valley Faults	CHV
Chalk Mountain Fault	CLK
Clayton—Montezuma Valley Fault	CLMV
Cedar Mountain Fault	CM
Checkpoint Pass Fault	CP
Central Pintwater Range Faults	CPR

Fault Name	Fault Abbreviation
Central Reveille Fault	CR
Cockeyed Ridge—Papoose Lake Fault	CRPL
Clayton Ridge—Paymaster Ridge Fault	CRPR
Cactus Range—Wellington Hills Fault	CRWH
Cane Spring Fault	CS
Central Spring Mountains Faults	CSM
Clayton Valley Fault	CV
Deep Springs Fault	DS
Death Valley Fault	DV
East Belted Range Fault	EBR
East Crater Flat Faults	ECR
Emigrant Fault	EM
East Magruder Mountain Fault	EMM
East Nopah Fault	EN
Emigrant Peak Faults	EPK
East Pintwater Range Fault	EPR
Eleana Range Fault	ER
East Reveille Fault	ERV
East Stone Cabin Fault	ESC
Eureka Valley East Fault	EURE
Eureka Valley West Fault	EURW
Emigrant Valley North Fault	EVN
Emigrant Valley South Fault	EVS
Furnace Creek Fault	FC
Fallout Hills Faults	FH
Fish Lake Valley Fault	FLV
Frenchman Mountain Fault	FM
Freiburg Fault	FR

Fault Name	Fault Abbreviation
Fatigue Wash Fault	FW
Ghost Dance Fault	GD
Golden Gate Faults	GG
Grapevine Mountains Fault	GM
Gold Flat Fault	GOL
Gold Mountain Fault	GOM
Groom Range Central Fault	GRC
Garden Valley Fault	GRD
Groom Range East Fault	GRE
General Thomas Hills Fault	GTH
Grapevine Fault	GV
Hot Creek—Reveille Fault	HCR
Hiko Fault	HKO
Hunter Mountain Fault	HM
Hiko—South Pahroc Faults	HSP
Hidden Valley—Sand Flat Faults	HVSF
Iron Ridge Fault*	IR
Indian Springs Valley Fault	ISV
Jumbled Hills Fault	JUM
Kawich Range Fault	KR
Kawich Valley Fault	KV
Keane Wonder Fault	KW
Lee Flat Fault	LEE
Little Lake Fault	LL
La Madre Fault	LMD
Lone Mountain Fault	LMT
Lida Valley Faults	LV
McAfee Canyon Fault	MAC

Fault Name	Fault Abbreviation
Monitor Hills East Fault	MHE
Monitor Hills West Fault	MHW
Mud Lake—Goldfield Hills Fault	MLGH
Mine Mountain Fault	MM
Montezuma Range Fault	MR
Monotony Valley Fault	MV
Midway Valley Fault*	MVF
North Desert Range Fault	NDR
Oak Spring Butte Faults	OAK
Oasis Valley Faults	OSV
Owens Valley Faults	OWV
Pahroc Fault	PAH
Panamint Valley Fault	PAN
Paintbrush Canyon Fault	PBC
Penoyer Fault	PEN
Pahranagat Fault	PGT
Pahute Mesa Faults	PM
Palmetto Mountains—Jackson Wash Fault	PMJW
Pahrump Fault	PRP
Pahrock Valley Faults	PV
Plutonium Valley—North Halfpint Range Fault	PVNH
Pagany Wash Fault*	PWF
Palmetto Wash Fault	PW
Quinn Canyon Fault	QC
Ranger Mountains Faults	RM
Racetrack Valley Faults	RTV
Rock Valley Fault	RV

Fault Name	Fault Abbreviation
Rocket Wash—Beatty Wash Fault	RWBW
Saline Valley Faults	SAL
Sheep Basin Fault	SB
Solitario Canyon Fault	SC
Stagecoach Road Fault	SCR
Southeast Coal Valley Fault	SCV
Southern Death Valley Fault	SDV
Sheep—East Desert Ranges Fault	SEDR
Sarcobatus Flat Fault	SF
Sheep Range Fault	SHR
Silver Peak Range Faults	SIL
State Line Fault	SL
Slate Ridge Faults	SL
Six-Mile Flat Fault	SMF
Sierra Nevada Fault	SNV
South Ridge Faults	SOU
Spotted Range Faults	SPR
Seaman Pass Fault	SPS
Stumble Fault	STM
Sever Wash Fault*	SW
Stonewall Flat Fault	SWF
Stonewall Mountain Fault	SWM
Sylvania Mountains Fault	SYL
Tem Piute Fault	TEM
Tikaboo Fault	TK
Tule Canyon Fault	TLC
Three Lakes Valley Fault	TLV
Tin Mountain Fault	TM

Fault Name	Fault Abbreviation
Tolicha Peak Fault	TOL
Towne Pass Fault	TP
Wahmonie Fault	WAH
Weepah Hills Fault	WH
Wilson Canyon Fault	WIL
West Pintwater Range Fault	WPR
West Railroad Fault	WR
West Spring Mountains Fault	WSM
Windy Wash Fault	WW
Yucca Fault	YC
Yucca Lake Fault	YCL
Yucca Wash Fault*	YWF

* Faults from Simonds et al. (1995)

Note: Faults alphabetized by fault abbreviation

TYPE 1 FAULTS IN THE YUCCA MOUNTAIN REGION